TRN: ZA8500294

MINTEK

# REPORT

## No. M58D

AN ELECTROCHEMICAL PROCESS FOR THE RECYCLING OF TUNGSTEN CARBIDE SCRAP

by

M.W. Johns

12th October, 1982
Reissued 30th July, 1984

COUNCIL FOR MINERAL TECHNOLOGY
200 Hans Strijdom Road
RANDBURG
South Africa

8

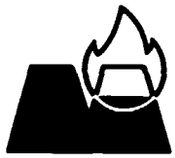

# MINTEK

(HYDROMETALLURGY DIVISION)

# REPORT
# No. M58D

## AN ELECTROCHEMICAL PROCESS FOR THE RECYCLING OF TUNGSTEN CARBIDE SCRAP

by

Mark William Johns

12th October, 1982
Reissued 30th July, 1984

Printed and published by the Council for Mineral Technology

ISBN 086999 681 9

Investigators R. Paul, W.A.M. te Riele, A. Bryson, M.W. Johns, W. Glatz, and H. Hegedus
Assistant Director of Division W.A.M. te Riele
Director of Division D.W. Boydell

Programme No. 009
Project No. 31179
Project Report No. 1

Sponsor Sandvik (Pty) Limited



All correspondence to Mintek, Private Bag X3015, Randburg, 2125 South Africa

## SYNOPSIS

An account is given of the development of a number of designs for electrochemical cells, and the subsequent construction and operation of a vibrating-plate cell capable of oxidizing 15 kilograms of tungsten carbide a day to a crude tungstic acid precipitate, with simultaneous recovery of cobalt metal on the cathode.

The effects on the process of the reagent concentration, temperature, current density, and cathode material are discussed.



## SAMEVATTING

Daar word verslag gedoen oor die ontwikkeling van 'n aantal ontwerpe vir elektrochemiese selle en die daaropvolgende konstruksie en werking van 'n vibreerplaatsel wat 15 kilogram wolframkarbied per dag tot 'n ruwe wolframsuurpresipitaat oksideer met gelyktydige herwinning van kobaltmetaal op die katode.

Die uitwerking van die reagenskonsentrasie, temperatuur, stroomdigtheid en katodemateriaal op die proses word bespreek.

## CONTENTS



## LIST OF TABLES

## LIST OF ILLUSTRATIONS

## 1. INTRODUCTION

The methods that are available for the recycling of cemented carbides can be separated into two classes. The first, based on the removal of the binder metal, leaves finely divided carbide, whereas the second involves chemical modification of the carbide. At the Council for Mineral Technology (Mintek) research into the recycling of tungsten carbide has been directed at the electrochemical oxidation of carbide. It has been shown[1] that the oxidation of carbide can be effected in a rotating titanium-drum anode immersed in 10 per cent (v/v) hydrochloric acid. Because of the problems encountered, however, it was decided that the oxidation of tungsten carbide in a sulphate medium should be investigated, with particular emphasis on the development of a process for the recovery of cobalt from solution.

This report describes the effects on the process of the concentration of reagents, temperature, current density, and cathode material, and the development of a number of designs for electrochemical cells. A pilot plant, in which approximately 15 kg of carbide was treated daily, was constructed and operated.

## 2. INITIAL TESTWORK

### 2.1. Equipment and Laboratory Procedures

Figure 1 shows the cell that was used. It consists of a drum anode, 12 cm long and 18 cm in diameter, mounted with its axis horizontal across an electrolyte tank of a capacity of 8 litres. The circular ends of the drums are of rigid PVC sheeting 10 mm thick, and the cylindrical wall of the drum is of titanium sheeting 1 mm thick perforated with holes 3 mm in diameter and 20 mm apart. Worn carbide drill bits for treatment are placed in the bottom of the drum and make electrical contact with the titanium. A small motor connected to the shaft at one end of the drum allows the drum to be rotated at various speeds.

A length of copper wire, suitably angled to fit inside the drum with one end protruding, was used as a cathode in the initial tests. This was later replaced by a stainless-steel plate (140 by 60 by 1 mm) suspended vertically in the electrolyte outside the drum. The immersed area of one side of the cathode was 50 $cm^2$.

Two carbides were tested: machine grade (90 per cent tungsten carbide, 10 per cent cobalt) and tool grade (70 per cent tungsten carbide, 10 per cent titanium carbide, 10 per cent tantalum carbide, 10 per cent cobalt). In all the tests, the mass ratio of machine-grade to tool-grade carbide loaded into the drum was 3:1.

The procedure followed for the testing of the cell was as follows. The electrolyte tank was filled with solution, and the drum containing the carbide was positioned in the tank. Power was connected across the drum and cathode, and the current was set. At the end of each run, the carbide that remained was weighed, as was the suspended tungstic acid recovered from the electrolyte. When the stainless-steel cathode was used, the cobalt that had formed on the cathode by electrodeposition was also weighed.

### 2.2. Results and Discussion

#### *2.2.1. Oxidation of Carbide*

As a test of whether tungsten carbide can be oxidized electrochemically in a sulphate medium without passivation of the cobalt, the drum was immersed in an electrolyte containing 10 g of sulphuric acid per litre and 30 g of ammonium sulphate per litre. Some worn carbide drill bits were placed in the drum, and a current of 3,8 A per 100 g was used. The cobalt concentration was continuously monitored, and is shown graphically in Figure 2. The points fall in a straight line, and indicate that passivation of the cobalt is unlikely. However, they fall below the theoretical line (the Appendix gives a calculation of the theoretical rate at which cobalt appears). The following two factors are suggested in explanation of this discrepancy.

(1) Evolution of oxygen. The current was measured across the empty anode drum. Upon calculation it was found that 93 per cent of the current was available for the oxidation of the carbide.

(2) The concentration of cobalt in the carbide. The theoretical rate was calculated for a constant 10 per cent in the carbide.

Further tests on the anodic dissolution of tungsten carbide are summarized in Table 1, and are discussed below.

*(1) Effect of Current Density*

At an average current density of 1,8 A per 100 g of carbide (Run G3), the measured value of mass lost through oxidation is greater than the theoretical value. This extra mass loss is largely due to the detachment of partially oxidized material caused by the milling action of the tumbling carbide bits. When the current density was increased (Runs G4 to G6), the values for mass loss of carbide, mass of tungstic acid residue, and percentage of acid soluble in ammonia were all very close to the theoretical values. The quantity of partially oxidized carbide present in the tungstic acid was significantly reduced. At a current density of 7,9 A per 100 g, the actual loss of mass was less than

the theoretical owing to some of the current being used for the evolution of oxygen, as can be seen from the Appendix.

*(2) Effect of Temperature*

The results indicate that the anodic dissolution of carbide is not sensitive to temperature.

*(3) Effect of Acid Concentration*

Doubling of the acid concentration had little effect on the results (Runs G4 and G5).

*(4) The Effect of Cobalt Concentration*

The effect of cobalt concentration could not be ascertained because the results of duplicate experiments were not adequately reproducible, but the effect, if any, appears to be small.

TABLE 1

*Results of anodic dissolution of tungsten carbide*

| | Run | | | | | | | |
|---|---|---|---|---|---|---|---|---|
| | G3 | G4 | G5 | G6 | G7 | G8 | G9 | G10 |
| $(NH_4)_2SO_4$ g·l$^{-1}$ | 30 | 30 | 30 | 30 | 30 | 30 | 30 | 30 |
| $H_2SO_4$, g·l$^{-1}$ | 10 | 10 | 20 | 20 | 18 | 21 | 21 | 20 |
| $Co^{2+}$, g·l | 3,4 | 3,3 | 3,8 | 3,8 | 4,2 | 5,4 | 30 | 30 |
| Total current, A | 6 | 12 | 20 | 20 | 20 | 20 | 20 | 20 |
| Current density, A·(100 g)$^{-1}$ | 1,8 | 3,8 | 3,9 | 4,7 | 7,9 | 4,3 | 4,3 | 4,3 |
| Time, h | 19 | 9,5 | 5,7 | 5,7 | 5,7 | 5,7 | 5,7 | 5,7 |
| Loss of mass, g | 88,8 | 80,1 | 80,9 | 80,1 | 75,8 | 84,1 | 90,0 | 78,5 |
| Mass of residue, g | 85,4 | 89,1 | 90,5 | 92,2 | 95,8 | 98,8 | 95,0 | 74,0 |
| $NH_3$ soluble, % | 85,4 | 89,8 | 91,8 | 90,0 | 89,9 | 91,5 | 89,6 | 85,0 |
| Cell voltage, V | 9 | 15 | 17 | 17 | 22 | 17 | 17 | 17 |
| Current (drum empty), A | 0,25 | 0,5 | 0,75 | 0,75 | 1,5 | 0,75 | 0,75 | 0,75 |
| Temperature, °C | 25 | 43 | 53 | 34 | 35 | 53 | 53 | 53 |

Conditions:
Mass ratio of machine-grade to tool-grade carbide 3:1
Rotary speed 25 r/min
Titanium-drum anode

### 2.2.2. Purity of the Products

The fine tungstic acid in the electrolyte was flocculated and filtered, and the cake was subjected to an ammonia leach to dissolve the tungstic acid. The insoluble component thought to be merely titanium dioxide and tantalum oxide was submitted for X-ray analysis. The phases identified in this analysis were tungsten carbide, titanium carbide, and tantalum carbide. No X-ray peak caused by any of the expected oxide compounds was found, suggesting that these are present in an amorphous form.

After leaching, the ammonia solution that was obtained contained cobalt at a level of 0,47 per cent. The attempted removal of cobalt from the crude tungstic acid sludge by treatment with 1 M sulphuric acid prior to the ammonia leach was unsuccessful. When the sulphuric acid and sludge were heated to approximately 60 °C and 1 ml of hydrogen peroxide was added for every 10 g of residue, the ammonia-soluble cobalt was completely removed.

The results of qualitative spectrographic analyses on the intermediate products are shown in Table 2. The cold sulphuric acid leach did not extract cobalt from the residue, but cobalt was successfully removed from the tungstic acid by a leach of hot sulphuric acid and hydrogen peroxide (Leach 5, Table 2). This ammonia leaching solution is pure enough to produce ammonium paratungstate (APT). APT was produced by the boiling of the leach liquor and removal of the APT crystals, which were heated in a porcelain crucible and yielded tungstic oxide of high quality.

### 2.2.3. Recovery of Cobalt

The recovery of cobalt from sulphate media by solvent extraction or ion exchange is difficult because either process has relatively poor selectivity for cobalt. Cobalt can be electrowon in the same cell as that in which carbide oxidation occurs. The current due to the deposition of cobalt at the cathode should equal the partial current for cobalt oxidation from the carbide. The mass of cobalt deposited at the cathode will

## TABLE 2

*Spectrographic analysis of the products of Run G8*

1. Tungstic acid produced from carbide oxidation
2. $H_2SO_4$ leaching solution
3. $H_2SO_4/H_2O_2$ leaching solution
4. $NH_3$ leaching solution (tungstic acid leached with $H_2SO_4$)
5. $NH_3$ leaching solution (tungstic acid leached with $H_2SO_4$ and $H_2O_2$)
6. Residue from $NH_3$ leach (from $H_2SO_4$ leach)
7. Residue from $NH_3$ leach (from a leach of $H_2SO_4$ and $H_2O_2$)

| Element | 1 | 2 | 3 | 4 | 5 | 6 | 7 |
|---|---|---|---|---|---|---|---|
| Ag | TVW | | | | | VW | VW |
| Al | VW | | | | | VWW | VWW |
| B | | | | VW | VW | W | W |
| Ca | VW | | | TVW | FT | VWW | VWW |
| Co | MS | VWW | WM | WM | VW | MS | MS |
| Cr | VWW | | | | | W | W |
| Cu | VWW | FT | VW | T | T | W | VW |
| Fe | VW | | | | | VW | VW |
| Hg | x | x | x | x | x | x | x |
| Li | x | x | x | x | x | x | x |
| Mg | VWW | T | T | TVW | T | VWW | VWW |
| Mn | T | | | | | VW | TVW |
| Mo | VW | | | WM | WM | VW | VW |
| Nb | WM | | | | | S | S |
| Ni | T | | | VW | | T | |
| Pb | VW | | | | | W | W |
| Si | VW | | | FT | FT | W | W |
| Sn | | | | | | W | W |
| Ta | M | | | | | S | S |
| Te | x | x | x | x | x | x | x |
| Ti | VS | | M | | | VS | VS |
| W | VS | | | VS | VS | VS | VS |

More than 1%, i.e.,

| | |
|---|---|
| VS | Very strong |
| S | Strong |
| MS | Moderately strong |

1 to 0,01%, i.e.,

| | |
|---|---|
| M | Moderate |
| W | Weak |
| VWW | Very weak to weak |

Less than 0,01%, i.e.,

| | |
|---|---|
| VW | Very weak |
| TVW | Traces to very weak |
| T | Traces |
| FT | Faint traces |

x Identification uncertain owing to interference from another element.

then exactly balance the mass of cobalt released into the electrolyte from the carbide, and the cobalt in solution will remain constant.

Preliminary tests were carried out to show the current efficiency for the deposition of cobalt onto a 1 $cm^2$ platinum electrode as a function of current density and electrolyte composition. The procedure involved the deposition, at constant current, of cobalt from the desired electrolyte at the required current density. The current efficiencies are listed in Table 3. These results are unlikely to apply directly to the electrowinning of cobalt on a very much larger scale, but they show an important trend that will probably apply to larger cathodes. The current efficiencies are very strongly dependent on acid concentration, decreasing with increasing acid concentration at any cobalt concentration and current density. Similarly, the current efficiencies increase strongly with increases in the cobalt concentration.

## TABLE 3

*The concentrations of cobalt and sulphuric acid required for the achievement of various current efficiencies*

| Current efficiency A·m$^{-2}$ | $Co^{2+}$ g·l$^{-1}$ | $H_2SO_4$ g·l$^{-1}$ | | | |
|---|---|---|---|---|---|
| | | Run 1 | Run 2 | Run 3 | Run 4 |
| −500 | 2 | 40 | 31 | 11 | 0,4 |
| −1000 | | 33 | 29 | 15 | 3 |
| −1500 | | 30 | 27 | 19 | 6 |
| −2000 | | 25 | 24 | 16 | 5 |
| −500 | 5 | 59 | 43 | 21 | 7 |
| −1000 | | 60 | 50 | 26 | 8 |
| −1500 | | 60 | 48 | 33 | 12 |
| −2000 | | 57 | 43 | 33 | 14 |
| −500 | 10 | 13 | 61 | 26 | 5 |
| −1000 | | 66 | 65 | 37 | 11 |
| −1500 | | 65 | 65 | 40 | 16 |
| −2000 | | 65 | 65 | 45 | 19 |

Conditions:
Platinum electrode in $(NH_4)_2SO_4$ 20 g·l$^{-1}$ containing various concentrations of $Co^{2+}$ and $H_2SO_4$

The cathode used was a stainless-steel sheet suspended in the electrolyte. The two competing cathodic reactions are the deposition of cobalt and the evolution of hydrogen. If the conditions are correctly chosen initially, the partial current due to the oxidation of the cobalt in the anode will be equal to the current efficiency at the cathode. If this balance is achieved, the acid concentration and the cobalt concentration in the electrolyte will remain unchanged during the electrolysis. If the current efficiency falls below 6,6 per cent, then the cobalt concentration in the electrolyte will increase and the acid concentration will decrease. The change in relative concentrations will cause the current efficiency to increase, which, in turn, will result in the cobalt and acid concentrations returning to their original values. Similarly, an increase in the current efficiency will be rectified, and thus the entire system is self-regulatory.

### *2.2.4. Combined Dissolution and Deposition of Cobalt*

The results obtained from the use of a cathode (total surface area 100 cm$^2$) positioned just outside the drum anode are shown in Table 4, but some additional details are as follows.

(1) The cathodes used during Runs G14 to G16 were placed inside porous polypropylene bags. It was hoped that this would prevent the occlusion of fine tungstic acid into the cobalt deposit, but it was not successful.

(2) During Runs G22 and G24, two stainless-steel cathodes were positioned side by side in the tank, thereby reducing the cathodic current density from 1500 A·m$^{-2}$ to 750 A·m$^{-2}$.

(3) A titanium cathode was used during Run G25.

(4) Two titanium cathodes were used during Run G26.

The measured values for mass losses of the carbide and for masses of tungstic acid were very close to the theoretical values. The percentage value of the tungstic acid soluble in ammonia was about 10 per cent less than the theoretical value.

The cathodic deposition of cobalt also appeared to work well. The mass of cobalt that should be plated for a constant concentration of $Co^{2+}$ in solution is 10 per cent of the mass of carbide lost. The sulphuric acid and cobalt concentrations remained reasonably constant at about 6 and 9,5 g·l$^{-1}$ respectively. Exceptions were Runs G22 and G26, in which the masses of cobalt were considerably lower (13,7 and 11,5 g). In both these tests the current density at the cathode was only 750 A·m$^{-2}$, but this drop in current efficiency was foreseen from the results in Table 3. It is interesting to note that the acid concentration at the start of Run G22, 6,4 g·l$^{-1}$, fell to 5,3 g·l$^{-1}$ by the end of the test, indicating an increase in the concentration

## TABLE 4

*Anodic dissolution of tungsten carbide and the deposition of cobalt*

| Property | Run | | | | | | | | | | |
|---|---|---|---|---|---|---|---|---|---|---|---|
| | G16 | G17 | G18 | G19 | G20 | G21 | G22 | G23 | G24 | G25 | G26 |
| Current, A | 13 | 13 | 13 | 15 | 15 | 15 | 15 | 15 | 15 | 15 | 15 |
| Time, h | 20 | 20 | 20 | 20 | 20 | 20 | 20 | 20 | 20 | 20 | 20 |
| Mass loss, g | 198 | 186 | 184 | 211 | 209 | 217 | 192 | 222 | 223 | 205 | 212 |
| Loss of residue, g | 198 | 193 | 198 | 236 | 234 | 243 | 231 | - | 213 | 268 | 189 |
| $NH_3$ soluble, % | 85 | 87 | 90 | 77 | 84 | 85 | 83 | 86 | 83 | 84 | - |
| Mass of Co deposited, g | 17,8 | 13,9 | 15,9 | 19,4 | 20,3 | 20,5 | 13,7 | 30,1 | 22,2 | 26,3 | 11,5 |
| Co purity, % | 79,5 | 76,5 | 75,5 | 70,0 | 74,0 | 72,0 | 62,3 | - | - | - | - |
| $(NH_4)_2SO_4$, $g\cdot l^{-1}$ | 40 | 40 | 40 | 40 | 40 | 40 | 40 | 120 | 120 | 120 | 120 |
| $H_2SO_4$ (start), $g\cdot l^{-1}$ | 5,8 | 6,3 | 4,5 | 6,5 | 6,3 | 6,2 | 6,2 | 5,0 | - | 7,0 | 8,5 |
| $H_2SO_4$ (end, $g\cdot l^{-1}$ | 6,1 | 6,4 | 7,0 | 6,9 | 6,1 | 5,7 | 5,3 | 7,0 | - | 8,6 | - |
| $Co^{2+}$ (start), $g\cdot l^{-1}$ | 9,2 | 10,0 | 10,0 | 9,4 | 9,8 | 9,5 | 9,7 | 9,5 | - | 9,3 | 9,3 |
| $Co^{2+}$ (end), $g\cdot l^{-1}$ | 9,5 | 0,0 | 8,7 | 8,8 | 9,6 | 9,3 | 9,7 | 9,2 | - | 9,3 | 9,3 |
| Cell voltage, V | 30 | 30 | 30 | 25 | 25 | 25 | 20 | 17 | 14 | 15 | 13 |

Note.
The theoretical loss of mass, mass of tungstic acid residue, and percentage extraction of ammonia for Runs G14, and G19 to G26, were 211 g, 242 g, and 94 per cent respectively. For Runs G16 to G18, they were 183 g, 210 g, and 94 per cent, respectively.
The initial mass of carbide in each experiment was 500 g.

of $Co^{2+}$ in the electrolyte. It could be expected therefore, that the current efficiency during Run G23 would be considerably higher, resulting in the plating of extra cobalt on the cathode. The measured mass of 30,1 g of cobalt plated during Run G23 effectively illustrates the self-regulatory nature of the process. Furthermore, it can be noted that the sulphuric acid regained its initial concentration of 7 $g\cdot l^{-1}$ by the end of Run G23.

The purity of the deposited cobalt was lower than had been expected. As the major impurities were tungsten, titanium, and iron, it seems likely that some of the finely divided tungstic acid and titanium dioxide suspended in the electrolyte was occluded in the deposit. Cobalt produced from Run G18 was ground to a powder and transferred to a beaker. A magnet below the beaker retained the cobalt, whereas the non-magnetic fraction was washed away. The washed cobalt (87 per cent of the original mass) analysed as 92 per cent pure.

The deposited cobalt was very poor. An increase in the ammonium sulphate concentration from 40 to 120 $g\cdot l^{-1}$ appeared to improve the deposit as well as to reduce the overall cell voltage. The best deposit was obtained with a titanium cathode, but the cobalt was so adherent that it could not be stripped from the titanium.

## 3. TESTING OF ALTERNATIVE CELL DESIGNS

Further testwork was undertaken with a view to the development of a simpler and cheaper cell. The two types built and tested were an oscillating trough and a vibrating perforated tray.

### 3.1. Design and Operation of Cells

#### *3.1.1. The Oscillating Trough*

Figure 3 is a schematic diagram of the oscillating trough, the design of which differs slightly from that of the rotary drum. It offers savings in both capital and operating costs. The advantages include the use of less titanium, the elimination of sliprings and perforations, the use of less power because of the short distance between the anode and cathode, and ease of access.

The trough is shaped like a half cylinder sliced along its axis (Figure 3), the cell having a diameter of 260 mm and a length of 250 mm. The sides of the trough are built up at an angle of 60° towards the centre for a distance of 55 mm (Figure 4). The angle of oscillation is adjusted by a crank-and-cam arrangement driven through a variable gearbox. Electrolyte is pumped into the cell at one end and leaves through two overflow weirs at the other, and this ensures that particles of tungstic acid are removed continuously. The unit is housed in a tank in which the bulk of the tungstic acid is allowed to settle. A curved stainless-steel plate positioned immediately above the drill bits acts as the cathode.

### 3.1.2. The Vibrating Perforated Plate

A perforated titanium plate is mounted horizontally in a tank, which is then vibrated by a vibratory feeder mechanism (Figure 5). Carbide drill bits are placed on the titanium plate, which serves as the anode, and the vibrating motion provides sufficient movement of the carbide to prevent passivation. Continuous removal of the particles of tungstic acid is achieved by the circulation of electrolyte across the anode. The perforations ensure that no tungstic acid remains trapped below the carbide bits, and a low edge serves to contain them on the plate. A stainless-steel plate acts as the cathode.

The vibrating perforated plate appears to offer considerable economic advantages over the rotating drum. These include the use of less titanium, simpler construction, lower power consumption due to the shorter distance between the anode and the cathode, and ease of scale-up.

## 3.2. Testwork

Tests were carried out on three different units as follows:

(1) a perforated rotary drum with an oscillating motion,

(2) an oscillating trough, and

(3) a vibrating perforated plate.

Machine-grade carbide scrap was used in all the tests.

### 3.2.1. Perforated Rotary Drum with Oscillating Motion

The movement of the drum was converted from a rotating to an oscillating motion, and the angle of oscillation could be adjusted by connection of the rod to different points on the cams. The speed of the drum was kept constant at 4 r/min.

The tests were designed to show the following:

(a) whether passivation due to the build-up of tungstic acid on the carbide bits could be prevented by oscillation of the drum,

(b) the effect of the angle of oscillation on passivation, and

(c) the decrease in cell voltage, and hence power consumption, when the cathode plate was placed inside the drum (Figure 6).

Four tests were carried out, each at an average current density of 4 A per 100 g of carbide bits. It was found that gradual passivation occurred at an angle of oscillation of 90°. Occasional vigorous shaking of the drum resulted in a sharp drop in the voltage. No passivation occurred at 110° and 140°. Table 5 shows that, in one test, the average voltage dropped to 11,5 V when the cathode was placed inside the drum.

TABLE 5

*Runs with oscillating cells on machine-grade material*

| Condition or result | Modified rotary drum | | | | Oscillating trough | | | | | |
|---|---|---|---|---|---|---|---|---|---|---|
| Run no. | 5 | 7 | 10 | 12 | OC/1 | OC/2 | OC/3A | OC/3B | OC/3C | OC/4 |
| Speed, r min | 4 | 4 | 4 | 4 | 4 | 4 | 4 | 4 | 4 | 4 |
| Angle of oscillation, degree | 90 | 140 | 110 | 110 | 110 | 87 | 112 | 112 | 112 | 112 |
| Duration of run, h | 21 | 22,5 | 19,5 | 25 | 66 | 25 | 15,8 | 38,1 | 6,8 | 27,4 |
| Average current, A | 20 | 20 | 20 | 20 | 36* | 27* | 36* | 16* | 35* | 38* |
| Average voltage, V | 21* | 14* | - | 11,5* | 11,5* | 14* | 11* | 13,5* | 12,5* | 11* |
| Current density, A per 100 g of drill bits | 4 | 4 | 4 | 4 | 1,79' | 1,37' | 1,80' | 0,80' | 1,76' | 1,92' |
| Current density at cathode, A·m$^{-2}$ | 2080 | 2220 | 2220 | - | 1753' | 1345' | 1767' | 781' | 1723' | 1885' |
| Drum charge, g | 500 | 500 | 500 | 500 | 2000 | 2000 | 2000 | 2000 | | 2000 |
| Bits dissolved, g·A$^{-1}$ per hour | 0,82 | 0,83 | 0,82 | 0,85 | 0,90 | 0,71 | 0,93 | 1,01 | | 0,65 |
| $H_2WO_4$ sludge formed, g·A$^{-1}$ per hour | 1,04 | 1,07 | - | 1,07 | 1,16 | 1,21 | 1,14 | 1,02 | | 0,65 |
| Location of cathode | Outside | Inside | Inside | Inside | - | - | - | - | | - |
| Solubility of ammonia, % | - | - | - | - | 96,8 | 98,5 | - | 98,2 | | 69,7 Tool bits |

* Average

' Limited by power supply

### 3.2.2. The Oscillating Trough

These tests were aimed at showing

(i) the mechanical reliability of the trough, and

(ii) a suitable angle of oscillation and flowrate of electrolyte.

The unit was run intermittently for 179 hours (Table 5) and operated satisfactorily as shown in Table 6. Passivation occurred when the angle of oscillation was reduced from 110 to 87°. Figure 7 shows the maximum current and voltages for Test OC/3, and it can be seen that the electrolyte must exceed a certain minimum flowrate if passivation due to the accumulation of tungstic acid in the cell is to be avoided.

The tungstic acid sludge produced from the drill bits was filtered, washed, and then dissolved in aqueous ammonia. Between 96,8 and 98,5 per cent dissolved. This figure dropped to 69,7 per cent for tool bits owing to the presence of insoluble compounds of titanium and tantalum.

TABLE 6

*Mass balance for oscillating trough, Run OC/4 (in grams)*

| | Constituents | Tungsten content | Cobalt content |
|---|---|---|---|
| *In* | | | |
| Bits at start | 2000,0 | 1314,2 | 200,0 |
| Bits added | 800,7 | 526,1 | 80,1 |
| Electrolyte | 9,5* | 151,2 | 140,6 |
| Total | | 1991,5 | 420,7 |
| *Out* | | | |
| Bits undissolved | 2126,2 | 1397,1 | 212,6 |
| Electrolyte | 8,58* | 213,1 | 134,7 |
| Tungstic acid | 678,3 | 383,9 | 14,3 |
| Cobalt | 45,4 | 8,7 | 28,1 |
| Total | | 2002,8 | 389,7 |
| Accountability, % | | 100,6 | 92,6 |

* Litres

### 3.2.3. The Vibrating Perforated Plate

During the preliminary runs, adjustments and modifications were made to the cell to eliminate operational problems. The following were the main problems:

(1) occasional short-circuiting due to the movement of partly corroded carbide bits that moved on top of larger bits,

(2) passivation due to incomplete removal of tungstic acid, and

(3) transportation of partly corroded carbide bits from the cell owing to the vibrating action.

A titanium mesh was placed over the anode basket to prevent excessive movement of the carbide bits. However, jamming occurred and resulted in gradual passivation and eventual tearing of the mesh. The following modifications greatly improved the operation.

(i) The perforated anode was raised slightly above the bottom of the tank so that circulating electrolyte could flow through the holes, thus removing tungstic acid sludge more effectively.

(ii) The tank was given a slight backward tilt to reduce the forward movement caused by the vibrator.

Longer runs were carried out as tests of the performance of the cell under different conditions, and so that estimates of scale-up parameters could be obtained. The anodic current density was varied from 1,33 to 6 A per 100 g carbide, and during each run fresh carbide bits were added periodically to keep the average inventory approximately constant. The cathodic current density was maintained at 2000 $A \cdot m^{-2}$, and cobalt was removed periodically from the cathode. The tungstic acid sludge was filtered, washed, dried, weighed, and its solubility in aqueous ammonia determined. The results are summarized in Table 7. The consumption of electrical energy was found to vary between 10 and 20 kW·h per kilogram of carbide, depending mainly on the anodic current density but also on the composition of the electrolyte. This was monitored, and it was found that the concentration of tungsten in the electrolyte rose gradually until it reached a level of approximately 50 $g \cdot l^{-1}$. The cobalt concentration showed a similar variation, rising to approximately 22 $g \cdot l^{-1}$. There was also a drop in the ammonia concentration in the electrolyte, probably affecting its conductivity. The mass balances for tungsten and cobalt are given in Table 8.

## TABLE 7

*Runs with a perforated vibrating plate on machine-grade material*

| Special features | Improved electrolyte circulation | | Larger vibrator, new cell | Sump added to cell | Anode tilted 10° | Anode tilted 6° | | | Anode tilted 6°, interruptions due to problems with rectifier | Anode plate lifted, fresh electrolyte | Anode–cathode gap varied during run | Anode–cathode gap varied during run | High current density, square cathode | High current density, rectangular cathode | Ammonia monitored |
|---|---|---|---|---|---|---|---|---|---|---|---|---|---|---|---|
| Condition or result | Run 14 | Run 15 | Run 16 | Run 17 | Run 18 | Run 19 | Run 20 | Run 21 | Run 23 | Run 24 | Run 25 | Run 27 | Run 28 | Run 29 | Run 30 |
| Vibrator speed, indicator setting | 10 | 10 | 2 | 2 | 2 | 2 | 2 | – | – | 1,5 | 1 to 1,5 | 1 to 2 | 1 | 1 | 0,5 to 1 |
| Duration of run, h | 5 | 4 | 6,5 | 8 | 12 | 12 | 12 | 74,5 | 118 | 178,5 | 233,5 | 235 | 12 | 12 | 95,25 |
| Average current, A | 20 | 20 | 20 | 20 | 20 | 20 | 10 | 20 | 20 | 20 | 20 | 20 | 28 | 29 | 20 |
| Average potential, V | 12 to 15 | 13 to 14 | 11 to 13 | 10 to 12 | 10 to 12 | 10 to 12 | 9 to 10 | 10 to 11 | 10 to 15 | 7 to 8 | 9 to 12 | 9 to 11 | 13 to 15 | 12 to 15 | 7 to 9 |
| Current density, $A \cdot 100 g^{-1}$ | 4 | 4 | 4 | 4 | 4 | 4 | 4 | 1,33 | 1,33 | 1,33 | 2,0 | 2,0 | 6 | 6 | 2,0 |
| Vibrating plate charge, g | 500 | 500 | 500 | 500 | 500 | 500 | 250 | 1500 | 1500 | 1500 | 1000 | 1000 | 500 | 500 | 1000 |
| Bits dissolved, $g \cdot A^{-1}$ per hour | 0,83 | 0,87 | 0,87 | 0,82 | 0,84 | 0,83 | 0,78 | 0,81 | 0,82 | 0,78 | 0,77 | 0,75 | 0,74 | 0,70 | 0,84 |
| Total amount of $H_2WO_4$ sludge formed, g | 112,1 | 81,8 | 145,1 | 158,0 | 263,7 | 278,8 | 118,2 | 1560,8 | 2222,4 | 2806,0 | 4213,2 | 4401,7 | 254,5 | 247,6 | 1694,1 |
| $H_2WO_4$ sludge formed, $g \cdot A^{-1}$ per hour | 1,12 | 0,82 | 1,15 | 0,99 | 1,10 | 1,13 | 0,99 | 1,05 | 0,94 | 0,79 | 0,90 | 0,94 | 0,51 | 0,74 | 0,69 |
| Pure $H_2WO_4$ formed, $g \cdot A^{-1}$ per hour | – | – | – | – | – | – | – | – | – | 0,87 | 0,93 | 0,85 | 0,83 | 0,77 | 0,95 |
| Cathode size, mm | – | – | 70 × 70 | 70 × 70 | 70 × 70 | – | – | 70 × 70 | – | 69 × 73<br>40 × 125 | 69 × 73 | 70 × 125 | 86 × 56 | 60 × 126 | 40 × 125 |
| Electrical energy consumed, $(kW \cdot h) \cdot kg^{-1}$ | 6,2 | 16,2 | 14,6 | 14,4 | 13,7 | 13,1 | 12,5 | 12,9 | 15,2 | 9,6 | 15,7 | 12,9 | 20,0 | 19,2 | 9,6 |
| Total amount of cathode deposit formed, g | – | 0,69 | – | 2,21 | – | – | – | – | – | 158,1 | 267,4 | 216,5 | 18,1 | 18,6 | 96,7 |
| Solubility of ammonia, % | – | 95,6 | 93,7 | – | 96,2 | 96,7 | 93,3 | 96,4 | 96,1 | 97,7 | 97,3 | 96,8 | 95,9 | 95,3 | – |

## TABLE 8

*Mass balances for runs with a vibrating plate (in grams)*

| Run no. | 24 | | 25 | | 27 | | 28 | | 29 | | 30 | |
|---|---|---|---|---|---|---|---|---|---|---|---|---|
| Element | W | Co | W | Co | W | Co | W | Co | W | Co | W | Co |
| *Input* | | | | | | | | | | | | |
| Bits at start | 1272,9 | 142,4 | 849,5 | 95,0 | 850,6 | 95,1 | 427,8 | 47,8 | 424,8 | 47,5 | 849,5 | 95,0 |
| Bits added | 3378,7 | 377,8 | 3208,3 | 358,8 | 3575,9 | 399,9 | 201,9 | 22,6 | 204,0 | 22,8 | 1273,1 | 142,4 |
| Electrolyte | - | - | 292,6 | 93,1 | 339,5 | 157,9 | 344,4 | 149,1 | 360,5 | 142,5 | - | - |
| Total | 4651,6 | 520,2 | 4350,4 | 546,9 | 4766,0 | 652,9 | 974,1 | 219,5 | 989,3 | 212,8 | 2122,6 | 237,4 |
| *Output* | | | | | | | | | | | | |
| Bits undissolved | 2286,3 | 255,7 | 1026,5 | 114,8 | 1322,8 | 147,9 | 433,5 | 48,5 | 431,6 | 48,3 | 767,2 | 85,8 |
| Electrolyte | 288,3 | 100,2 | 379,9 | 161,3 | 323,4 | 151,9 | 361,9 | 138,6 | 376,6 | 139,3 | 140,6 | 55,5 |
| $H_2WO_4$ sludge | 1969,8 | 28,9 | 3016,7 | 77,1 | 2909,5 | 160,2 | 169,4 | 9,6 | 170,0 | 6,4 | 1180,8 | 4,6 |
| Cobalt | 25,6 | 105,1 | 93,1 | 106,2 | 45,8 | 128,2 | 3,5 | 11,0 | 3,5 | 9,5 | 14,6 | 61,9 |
| Cathode cleaning | - | - | 0,1 | 2,9 | 4,6 | 2,1 | 0,1 | 1,1 | 0,1 | 1,1 | 0,2 | 0,9 |
| Total | 4570,0 | 489,9 | 4517,7 | 462,3 | 4606,1 | 590,3 | 968,4 | 208,8 | 981,8 | 204,6 | 2103,4 | 208,8 |
| Accountability, % | 98,2 | 94,2 | 103,8 | 84,5 | 96,6 | 90,4 | 99,4 | 95,1 | 99,2 | 96,2 | 99,1 | 87,9 |

The following observations were made in regard to the runs with the vibrating plate.

*(a) The Cooling of the Electrolyte by Evaporation and Cooling Cells*

Most of the electrical energy supplied to the cell is dissipated by resistive heating of the electrolyte. It was established that, at a cell temperature of 41 °C, the rate of evaporation per square metre of free surface was 1,82 l·h$^{-1}$. This increased to 3,02 l·h$^{-1}$ at 51 °C. Cooling water flowing through glass coils placed in the electrolyte removed some 40 per cent of the total energy input.

*(b) The Continuous Removal of Tungstic Acid Sludge*

When the solids content of circulating electrolyte was determined on a daily basis for Run 25, the results showed that the solids content remained constant at approximately 18 g of sludge per litre. Hence, for drill bits, a settler area of 0,0079 m$^2$ is adequate for the production of 0,018 kg of sludge per hour.

*(c) The Recyling of Carbide Bits*

Despite the backward tilt of 9° and the presence of a weir 13 mm high, a small proportion of partially corroded carbide bits was transported out of the cell. These bits were easily recovered on a screen and were returned to the cell. For Runs 25 and 27, the recycling stream amounted to 8 and 9,6 per cent respectively.

*(d) The Loss of Ammonia*

Analysis of the electrolyte at the end of Run 7 showed that there had been an appreciable loss of ammonia: the concentration had dropped from 28 to 2,5 g·l$^{-1}$ over an operating period of 500 hours. For Run 30, fresh electrolyte was used and the concentration of ammonia was determined on a daily basis. Analysis of the washed sludge showed a concentration of between 2 and 2,4 per cent, which accounts for most of the ammonia lost from the electrolyte.

*(e) The Recovery of Cobalt from a Stainless-steel Cathode*

The grade of the cobalt produced was between 58 and 66 per cent. which is considerably lower than that obtained previously. The main contaminant was tungsten, and it was observed that, unless the deposit was removed from the cathode twice a day, dendritic growth prevented satisfactory operation.

*(f) The Gap between the Anode and the Cathode*

The distance between the anode and the cathode plates affects the cell voltage, and hence the power consumption. The shorter the distance, the lower the voltage. However, a short distance increases the chance of a short circuit by a direct contact between the carbide bits and the cathode. A safe minimum distance for drill bits was found by trial and error to be 22 mm.

*(g) The Loading of the Anode*

Carbide bits undergoing anodic oxidation require a certain freedom of movement on the vibrating plate if passivation is to be prevented. In one experiment, the anode was loaded to 8 g of tungsten

carbide per square centimetre and, after a short period of operation, passivation occurred. This is attributed to the fact that there was insufficient room available for the breakdown of tungstic acid flakes by the movement of the carbide bits. For drill bits, a safe anode loading was found to be 5 to 6 g of tungsten carbide per square centimetre.

## 4. PILOT-PLANT WORK

It was considered essential that further testwork should be undertaken on a pilot-plant scale before the process was operated on a commercial scale.

### 4.1. Design of a Vibrating-plate Cell

In the design of a vibrating-plate cell that could treat 15 kg of drill bits per day, the calculation of the anode area was based on the following design parameters:

| | |
|---|---|
| Anode current density | 4 A per 100 g of carbide |
| Anode loading (carbide) | 5,5 g·cm$^{-2}$ |
| Carbide conversion per hour | 0,8 g·A$^{-1}$. |

If the cell is operated continuously for 24 hours per day, the following current is required:

$$\frac{1500}{0{,}8 \times 24} = 781 \text{ A}.$$

Therefore, the cell inventory becomes

$$\frac{781 \times 100}{4 \times 1000} = 19{,}5 \text{ kg of carbide bits}.$$

This amount requires an anode area of

$$\frac{19{,}5 \times 1000}{5{,}5} = 3550 \text{ cm}^2.$$

A square anode (60 by 60 cm) was adopted for greater mechanical stability when the anode was attached to the vibrator. The plate (titanium) 3 mm thick, is perforated with holes of 1,5 mm diameter at a pitch of 10 mm, and is mounted in a rubber-lined mild-steel tank. Current was supplied to the plate at 18 points via studs through the bottom of the tank. A stainless-steel cathode (50 by 50 cm) was mounted at an adjustable distance above the anode. Details of the cell are shown in Figures 8 to 10, and a flowsheet of the pilot plant is given in Figure 11.

### 4.2. Initial Tests and Modifications

The cell was initially mounted on a vibratory feeder of the type used in the laboratory-scale work. Three models were tried, but they did not provide sufficient vibration, and the distribution of the bits on the anode was unsatisfactory. The cell appeared to be dynamically unstable, and four rods with rubber mountings were attached to the underside of the cell at each corner but this did not improve the performance. The vibratory feeder was then removed and mounted on the main frame as shown in Figure 10a. Two unbalanced motors were positioned on opposite sides of the cell. Although the cell was far more stable, the level of vibration was insufficient and the distribution of the bits on the anode was irreproducible. Two larger motors were tried, but the distribution of the bits was still unacceptable. When a single vibrator was mounted on the feed side of the cell and the whole structure was tilted through an angle of 2,2° (Figure 10b), there was a marked improvement. This arrangement resulted in some passivation of the anode, and a larger unbalanced motor (a Joest V 08001/4) with a lower vibration frequency eventually gave the required distribution.

Electrical short-circuiting of the cell by direct contact between the bits and the cathode during operation over lengthy periods was prevented by the provision of a nylon screen (ASTM 14-mesh) attached to the underside of the cathode.

A further problem concerned the trapping of hydrogen gas under the cathode plate, resulting in an unacceptably large voltage drop across the cell. Sixteen 6 mm holes were drilled 100 mm apart in the cathode, but this did not allow sufficient gas to escape. The problem was solved when the cathode sheet was replaced with a stainless-steel wire mesh of 1,6 mm diameter wire with 3,2 mm square openings.

### 4.3. Continuous Pilot-plant Runs

Three continuous pilot-plant runs, each of 90 hours duration, were completed. The general procedure during each run was as follows. A load of 25 kg of clean bits was placed on the anode, and the system was filled with 175 litres of electrolyte. The plant was then started, and the temperature, voltage, and amperage were monitored. Bits were added at a rate of 0,8 kg/(1000 A) per hour, and ammonium sulphate was added to make up the ammonia lost in the sludge. After each shift, a clean cathode was fitted and the cobalt was scraped off the cathode that had been replaced. The coarse sludge was removed from the settler every 3 to 4 hours. At the end of the run, suspended sludge was filtered from the electrolyte, the fixed cobalt was removed from the cathodes by cleaning in hydrogen peroxide, and the tungstic acid on the surface of the bits was cleaned off in ammonia.

A summary of the average pilot-plant conditions for the three runs is given in Table 9, and the mass balances are shown in Tables 10 to 12. Figures 12 to 14 show the variation in the concentrations of cobalt and tungsten in the electrolyte for the three runs, and Figure 15 depicts the rate of the build-up of solids in suspension. Figure 16 shows the variation in the voltage with respect to time.

TABLE 9

*Average pilot-plant conditions*

| Operating conditions | Run 12P | Run 13P | Run 14P |
|---|---|---|---|
| Length of run, h | 92,42 | 93,24 | 92,62 |
| Cathode changed, every no. of h | 12 | 8 | 8 |
| Current, A | 760 | 800 | 800 |
| Voltage, V | 9,0 | 8,6 | 9,2 |
| Temperature at which cell overflowed, °C | 50,0 | 48,7 | 47,8 |
| Bits treated, kg/d | 14,3 | 15,7 | 15,4 |
| Sludge produced, kg/d | 17,6 | 19,4 | 19,3 |
| Co deposited, kg/d | 0,88 | 1,41 | 1,25 |
| $NH_3$ consumed, kg/d | 0,417 | 0,559 | 0,540 |
| Cooling water per kg of bits treated, litre | 366,5 | 187,0 | 523,3 |
| Make up water per kg of bits treated, litre | 2,6 | 6,2 | 2,8 |
| Amps consumed per kg of bits treated, A·h $^{-1}$ | 1244 | 1208 | 1236 |
| Energy consumed per kg of bits treated, kW·h | 11,5 | 10,4 | 11,4 |

#### *4.3.1. Run 12P*

With respect to the electrolyte concentration (Figure 12), the cobalt concentration levelled out to 17 g·l $^{-1}$ but the tungsten still declined, being 12 g·l $^{-1}$ at the end of the run. The acid concentration was reasonably steady between 8 and 9 g·l $^{-1}$. Four additions of ammonium sulphate were necessary, the first two being start-up adjustments. The mass balance (Table 10) showed a high accountability for tungsten and a low accountability for cobalt.

The major problem during this run was an increase in the suspended solids of the electrolyte from almost zero at the start of the run to 110 g·l $^{-1}$ at the end (Figure 15). A further problem resulted from the formation of cobalt dendrites on the cathode in that some of these became detached before the stripping and reported in the tungstic acid sludge.

TABLE 10

*Mass balance for Run 12P (in grams)*

| Description | Mass, kg | | | |
|---|---|---|---|---|
| | Total | W | Co | $NH_3$ |
| *Input* | | | | |
| Bits, starting charge | 25,000 | | | |
| Bits added | 54,417 | | | |
| Bits remained | 24,432 | | | |
| Bits dissolved | 54,985 | 46,710 | 5,224 | |
| Electrolyte | 175* | 4,305 | 2,397 | 2,765 |
| $(NH_4)_2SO_4$ added | 14 | | | 3,609 |
| Total | | 51,015 | 7,621 | 6,374 |
| *Output* | | | | |
| Tungstic acid sludge | 67,604 | 47,864 | 0,744 | 1,555 |
| Cobalt deposit | 3,384 | 0,636 | 2,352 | 0,015 |
| Cathode-cleaning solution | 3,66* | 0,021 | 0,088 | |
| Bits-cleaning solution | 2,39* | 0,122 | 0,001 | |
| Electrolyte and wash water | 213* | 3,046 | 3,280 | 4,729 |
| Total | | 51,629 | 6,465 | 6,299 |
| Accountability, % | | 101,3 | 84,8 | 98,8 |

Bits assumed to contain 90,5% WC and 9,5% Co.
* Litres

TABLE 11

*Mass balance for Run 13P (in grams)*

| Description | Mass, kg | | | |
|---|---|---|---|---|
| | Total | W | Co | $NH_3$ |
| *Input* | | | | |
| Bits starting charge | 25,000 | | | |
| Bits added | 58,424 | | | |
| Bits remaining | 22,587 | | | |
| Bits dissolved | 60,837 | 51,683 | 5,780 | |
| Electrolyte | 280* | 3,276 | 2,500 | 6,720 |
| $(NH_4)_2SO_4$ added | 9,8 | | | 2,423 |
| Total | | 54,959 | 8,280 | 9,143 |
| *Output* | | | | |
| Tungstic acid sludge | 75,262 | 49,297 | 0,369 | 2,514 |
| Cobalt deposit | 5,472 | 0,979 | 3,858 | 0,025 |
| Cathode-cleaning solution | 7,00* | 0,080 | 0,123 | |
| Electrolyte and wash water | 297* | 3,481 | 3,475 | 7,336 |
| Bits-cleaning solution | 2,22* | 0,061 | 0,001 | |
| Total | | 53,898 | 7,826 | 9,875 |
| Accountability, % | | 98,1% | 94,5% | 108,0% |

Bits assumed to contain 90,5% WC and 9,5% Co.
* Litres

## TABLE 12

*Mass balance for Run 14P (in grams)*

| Description | Mass, kg | | | |
|---|---|---|---|---|
| | Total | W | Co | $NH_3$ |
| ***Input*** | | | | |
| Bits, starting charge | 25,001 | | | |
| Bits added | 58,400 | | | |
| Bits remaining | 24,090 | | | |
| Bits dissolved | 59,311 | 50,386 | 5,635 | |
| Electrolyte | 220* | 2,508 | 2,508 | 5,874 |
| $(NH_4)_2SO_4$ added | 7,5 | | | 1,934 |
| Total | | 52,894 | 8,143 | 7,808 |
| ***Output*** | | | | |
| Tungstic acid sludge | 74,40 | 45,905 | 0,789 | 2,046 |
| Cobalt deposit | 4,835 | 0,900 | 3,007 | 0,022 |
| Cathode, cleaning solution | 9,72* | 0,033 | 0,094 | |
| Electrolyte and wash water | 233* | 1,892 | 2,516 | 5,709 |
| Bits, cleaning solution | 1,87* | 0,002 | | |
| Total | | 48,861 | 6,408 | 7,777 |
| Accountability, % | | 92,4 | 78,7 | 99,6 |

Bits assumed to contain 90,5% WC and 9,5% Co.
* Litres

### 4.3.2. Run 13P

The following modifications were made before Run 13P with the purpose of improved performance.

(1) As the stainless-steel mesh used for the cathode had proved to be weak, it was replaced with stronger mesh. The screen had a wire diameter of 3 mm and square openings of 5 mm. The substitution gave an increase of 44 per cent in the surface area available for the plating out of the cobalt.

(2) Because of the cobalt dendrites that formed on the cathode and became lost in the tungstic acid sludge, the cathodes were changed every 8 hours, instead of every 12 hours as in Run 12P.

(3) The size of the 28 spray holes used in the washing of the top surface of the anode was increased from 2 to 5 mm to provide better washing over the anode and thus prevent a build-up of tungstic acid above the bits.

(4) The 55-litre settler was replaced with a 175-litre settler so that the concentration of solids suspended in the electrolyte would be reduced.

Figure 13 shows the concentration profile of the electrolyte. The tungsten concentration varied between 11 and 16 g·l$^{-1}$, and the cobalt rose continuously to 11 g·l$^{-1}$ and the acid to 12 g·l$^{-1}$. The mass balance (Table 11) showed good accountability.

The problems encountered during Run 13P were as follows.

(i) As shown in Figure 15, the level of suspended solids for Run 13P was considerably lower than that for Run 12P. However, completely steady state was not reached, and the level varied somewhat randomly. This was probably due to occasional surging of the electrolyte between the cell and the settler.

(ii) Removal of the settled sludge at the bottom of the settler proved difficult.

(iii) The sludge transferred through the holes in the anode was not removed efficiently, and there was an accumulation of solids on the cell floor.

### 4.3.3. Run 14P

The following further modifications were made to the cell.

(1) Beneath the anode, a polyethylene plate 30 mm thick was installed at an angle of 2,4° to the bottom of the cell to prevent a build-up of tungstic acid sludge.

(2) A smaller settler was used because of its ease of operation. A removable plug was introduced at the bottom of the settler to facilitate the removal of sludge.

The fine sludge suspended in the solution was removed as follows. After each 8-hour shift, the plant was stopped and 50 litres of the electrolyte was removed into a tank. The electrolyte was allowed to settle for one shift. Supernatant liquor from the electrolyte that had been drained off at the end of the previous shift was then returned to the plant. As shown in Figure 15, the rate of build-up of suspended solids was higher than expected (0,83 $g \cdot l^{-1}$ per hour). Further tests have shown that, with slight modification of the equipment used for draining off the supernatant liquor, the solids in suspension can be kept constant at a far lower concentration (Section 4.5).

The cobalt concentration during the run (Figure 14) reached 15 $g \cdot l^{-1}$, and the tungsten value dropped to 9 $g \cdot l^{-1}$. The mass balance (Table 12) does not show as good an accountability as those shown for the previous two runs (Tables 10 and 11).

The problems encountered during Run 14P were as follows.

(a) Harvesting of the cobalt, although easier than when the lighter cathode was used, was still difficult. The cobalt dendrites were easily removed, but complete removal of the cobalt plated onto the cathode was labour-intensive.

(b) The polyethylene plate seemed to dampen the vibrations, causing a degree of passivation and hence a higher average voltage (Table 9).

(c) Sludge trapped between the bits appeared to cause a widening of the voltage band. The bits on the anode were therefore raked before the cathode was lowered.

The following two points are worth noting from Figure 16, which shows the voltage profiles for each run.

(i) Between two successive shifts, i.e., when the cathodes were interchanged, there was a rise in the voltage. The reason for this is unknown.

(ii) During Runs 12P and 13P, the voltage stayed at a constant level, whereas during Run 14P a degree of passivation occurred, probably due to the introduction of the polyethylene plate.

### 4.4. Tests on Solids in Suspension

The effects on the solids in suspension of the gap between the anode and the cathode, the flow of electrolyte, and the size of the anode hole were investigated. Six short pilot-plant runs were done, of 6 to 7 hours each.

Table 13 contains the details of these runs, and Figure 17 shows a plot for the six runs of solids in suspension against time.

TABLE 13

*Pilot-plant runs on solids in suspension*

| Condition | 15P | 16P | 17P | 18P | 19P | 20P |
|---|---|---|---|---|---|---|
| Anode–cathode gap, mm | 20 | 50 | 35 | 35 | 35 | 35 |
| Diameter of perforated holes in anode, mm | 1,5 | 1,5 | 1,5 | 2,0 | 2,0 | 2,0 |
| Flowrate, $l \cdot min^{-1}$ | 45 | 45 | 45 | 45 | 67,5 | * |
| Length of run, h | 7 | 7 | 6 | 6 | 6 | 6 |
| Voltage, V | 7,9 to 8,9 | 11,9 to 13,3 | 10,1 to 11,6 | 9,6 to 11,2 | 9,8 to 11,3 | 8,9 to 10,2 |
| Current, A | 800 | 800 | 800 | 800 | 800 | 800 |
| Mass of $H_2WO_4$ trapped between bits, kg | 1,363 | 1,133 | 1,033 | 0,980 | 1,039 | 1,040 |
| Solids in suspension at time, $g \cdot l^{-1}$ | | | | | | |
| 0 h | 0,99 | 0,36 | 0,25 | 0,46 | 0,81 | 0,15 |
| 1½ h | | 0,97 | | | | |
| 3 h | 3,86 | | 1,16 | 0,92 | 1,70 | 0,79 |
| 6 h | | | 2,87 | 1,83 | 2,18 | 1,67 |
| 7 h | 6,72 | 3,43 | | | | |
| Hourly increase in solids in suspension, $g \cdot l^{-1}$ | 0,81 | 0,44 | 0,44 | 0,23 | 0,23 | 0,25 |

#### *4.4.1. Variation in Anode-Cathode Gap*

For Runs 15P, 16P, and 17P, all the parameters except the length of the anode–cathode gap were kept constant. An increase in the gap from 20 to 35 mm decreased the rate of solids build-up from 0,81 to 0,44 g·l$^{-1}$ per hour, but a further increase to 50 mm had no effect on the rate. For each of these increases in the gap, the voltage increased by about 2 V owing to the voltage drop in the electrolyte.

With a gap of 20 mm, the cathode impeded the flow across the anode, causing turbulence. At 35 and 50 mm no impedance occurred, and the flow patterns for these two settings were identical. A higher flowrate across the anode (when the gap is increased) resulted in the tungstic acid having a lower residence time on the anode, and there was therefore less grinding of the tungstic acid sludge between the bits. This prevented the solids from being ground into smaller sizes and hence reduced the rate at which the solids went into suspension.

The amount of solids trapped on the anode at the end of the run decreased, but not significantly.

#### *4.4.2. Diameter of the Holes in the Anode*

The size of two-thirds of the holes in the anode was increased from 1,5 to 2,0 mm before Run 18P so that blockage of the holes would be reduced and larger particles of sludge would be allowed to pass through the holes.

As can be seen from Figure 17, the rate of solids build-up between the two runs decreased from 0,44 to 0,23 g·l$^{-1}$ per hour. This showed that less grinding of the sludge had taken place.

#### *4.4.3. An Increase in the Flowrate*

For Run 19P the flowrate was increased by 50 per cent, in the hope that the sludge would be washed off the anode before it could be ground. However, the rate at which the solids went into suspension remained constant, indicating that the increased flowrate had had no effect.

#### *4.4.4. The Flow Pattern*

For Run 20P the cell was modified so that the electrolyte flowed upwards through the holes in the anode. It was hoped that this would wash away the sludge trapped between the bits. However, as can be seen from Table 13, the amount of sludge on the anode at the end of the run was not significantly different from that of the previous runs.

#### *4.4.5. Particle-size Distribution*

For each run, two samples of electrolyte were taken: one during the run and one at the end. The particle-size distribution of the associated solids was then measured. Figure 18 shows histograms of the particle size for Runs 15P and 18P.

Two points can be noted.

(1) The mass of solids in the smaller size ranges decreased dramatically after the changes.

(2) The 50 percentile (i.e., the size below which 50 per cent by mass of the particles fell) increased from 3 to 5 $\mu$m, and the electrolyte slurry therefore settled more easily.

### 4.5. Batch Settling Tests

A sample of electrolyte was allowed to settle under gravity, and particle-size analyses were done on samples taken periodically. It was found that the mass fraction of suspended solids decreased with time, but the 50 percentile remained constant at 4,7 $\mu$m. According to Stokes' Law, if free settling had occurred, the 50 percentile should have decreased with time. As this had not happened, it was concluded that natural agglomeration had occurred.

In flocculation tests on the electrolyte, five classes of flocculant were tested: anionic, cationic, neutral, guar-gum, and starch-based flocculants. Of these, the anionic flocculant produced the supernatant liquor of the highest clarity.

### 4.6. Purification of Tungstic Acid Sludge

#### *4.6.1. Magnetic Separation*

Tungstic acid sludge from Run 13P was ground to particles smaller than 208 $\mu$m and was then put through a high-intensity magnetic separator at two different voltage settings. The magnetic fraction and the original sample were analysed for tungsten and cobalt (Table 14). As can be seen, magnetic separation did not increase the cobalt content in the magnetic fraction, i.e. as the recovery decreased, the grade remained constant.

TABLE 14

*Results of high-intensity magnetic separation*

| | Mass % | CO % | W % |
|---|---|---|---|
| Head (original sample) | | 0,52 | 63,5 |
| Magnetic fraction at 8 V setting | 1,61 | 0,58 | 65,7 |
| Magnetic fraction at 15 V setting | 2,92 | 0,49 | 65,2 |

Two further tests were done, one with a finer sample and the other with a hand magnet. Neither of these tests was succesful.

### *4.6.2. Chemical Separation*

After much laboratory testwork, satisfactory results were achieved with the following procedure. Sludge was leached in a 1:1 solution of ammonium hydroxide at room temperature (solid-to-liquid ratio of 1 kg to 5 litres). After 30 minutes the slurry was removed from the stirred reactor and the insoluble material was filtered off. The filtrate was then heated and ammonium sulphide was added (in 100 per cent excess of the stoichiometric cobalt content). After stirring for 10 minutes, 1 g of charcoal was added to aid the filtration, and the sulphide residue was filtered off. The APT crystals were recovered from the filtrate by evaporative crystallization. Calcination at 600 °C for half an hour produced tungsten oxide for spectrographic analysis. Table 15 shows that tungsten oxide of excellent purity was achieved. The once-through recovery as tungsten oxide was 94 per cent (Table 16).

TABLE 15

*Impurity levels in tungsten trioxide*

| Impurity | Maximum allowable levels p.p.m. | Run 1 | Run 2 | Run 3 |
|---|---|---|---|---|
| Mo | 1000 | 30 | 35 | 10 |
| Fe | 300 | <10 | <10 | <10 |
| Na | 100 | <30 | <30 | <30 |
| K | 100 | | | |
| S | 100 | <100 | <100 | <100 |
| P | 80 | | | |
| As | 50 | 10 | <10 | <10 |
| Al | 20 | <10 | 10 | 11 |
| Si | 70 | <10 | <10 | <10 |
| Co | - | <10 | 12 | <10 |
| Cu | - | <30 | <30 | <30 |

Note.
The concentrations of antimony, nickel, zinc, bismuth, titanium, magnesium, lead, calcium, tin, and chromium were all below 10 p.p.m.

## 5. CONCLUSION

The tests showed that the electrochemical technique developed for the recycling of tungsten carbide scrap is successful in that tungstic acid sludge produced by the cell can be processed to tungsten oxide of high purity, and that the cell operated successfully on a continuous basis, treating 15 kg of scrap per day.

TABLE 16

*Mass balances for the purification of tungstic acid (in grams)*

| | Run 1 | | Run 2 | | Run 3 | |
|---|---|---|---|---|---|---|
| | Total | Tungsten | Total | Tungsten | Total | Tungsten |
| *Input* | | | | | | |
| Tungstic acid sludge | 100 | 65,50 | 100 | 70,50 | 1300 | 851,50 |
| *Output* | | | | | | |
| Insolubles, first filtration | 3,50 | 3,20 | 4,57 | 3,15 | 77,51 | 43,17 |
| Sulphide residue, second filtration | 2,49 | 0,06 | 1,23 | 0,04 | 34,68 | 6,97 |
| Filtrate after evaporative crystallization | 120* | 3,25 | 118* | 4,61 | 770* | 12,24 |
| $WO_3$ product | 74,33 | 58,94 | 76,82 | 60,92 | 1009,84 | 800,52 |
| Recovery, % | | 89,98 | | 86,41 | | 94,01 |
| Accountability, % | | 99,93 | | 97,48 | | 101,34 |

* Millilitres

## 6. REFERENCE

POWER, G.P., STAPLETON, W.M., and NICOL, M.J. National Institute for Metallurgy. Private Communication 1978.

Key:

- A Cylindrical sides of drum, constructed from 1 mm titanium, perforated with 3 mm holes positioned 20 mm apart
- B 8-litre tank
- C Shaft of drum
- D Electrolyte
- E Copper-wire cathode
- F Carbide bits
- G Stainless-steel cathode
- H Copper slip ring
- J Motor

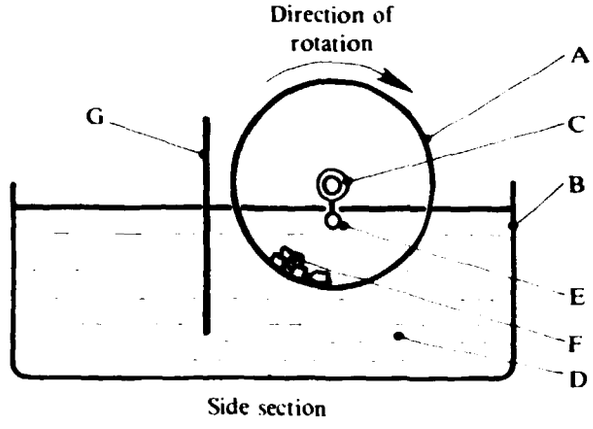


Side section

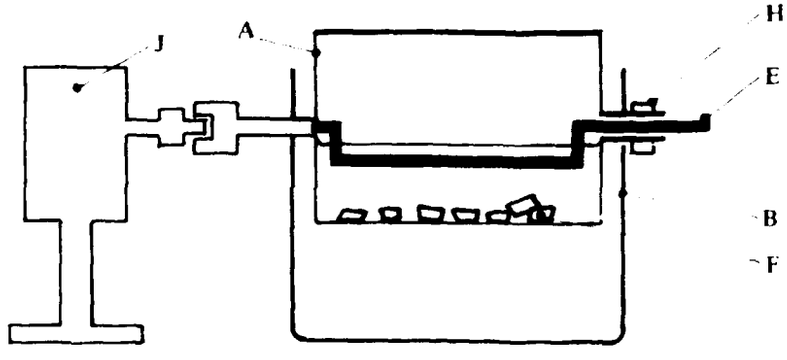


Front section

FIGURE 1. The rotating drum

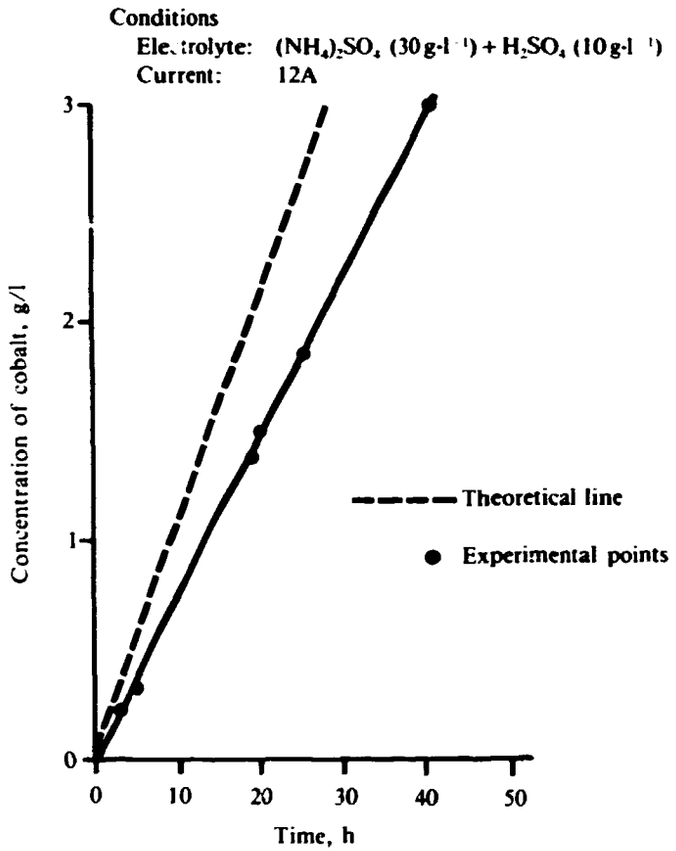


FIGURE 2. Rate of cobalt build-up

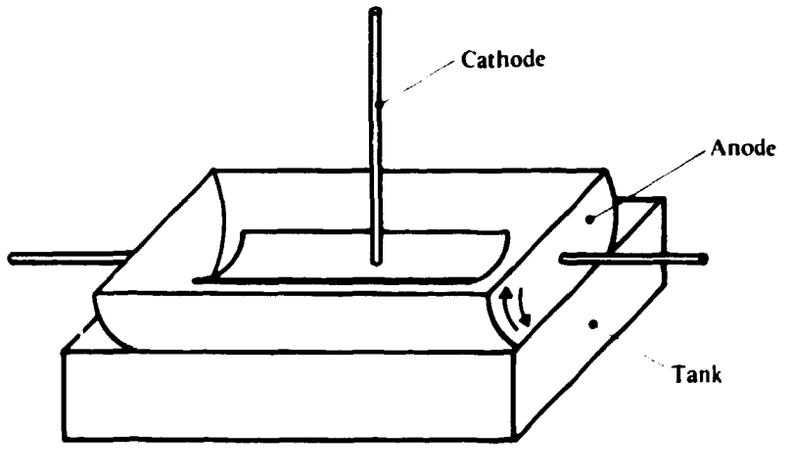


FIGURE 3. The oscillating trough

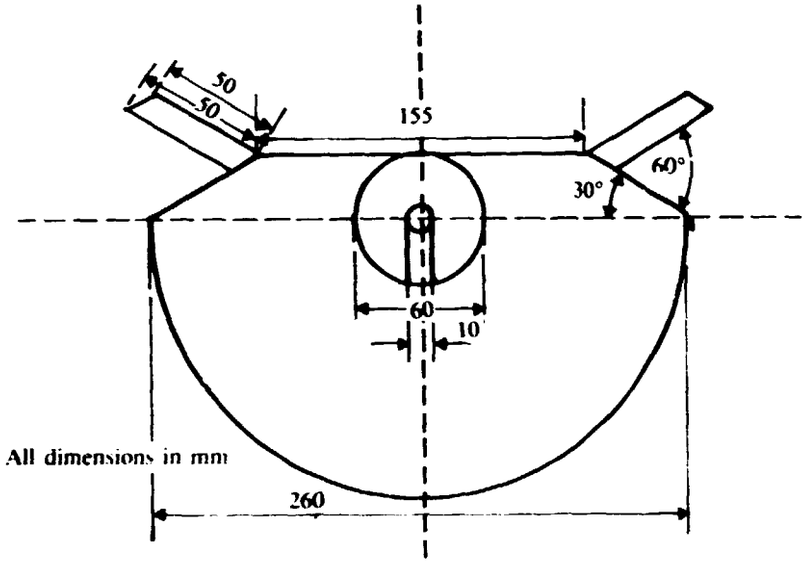


FIGURE 4. Side elevation of oscillating trough

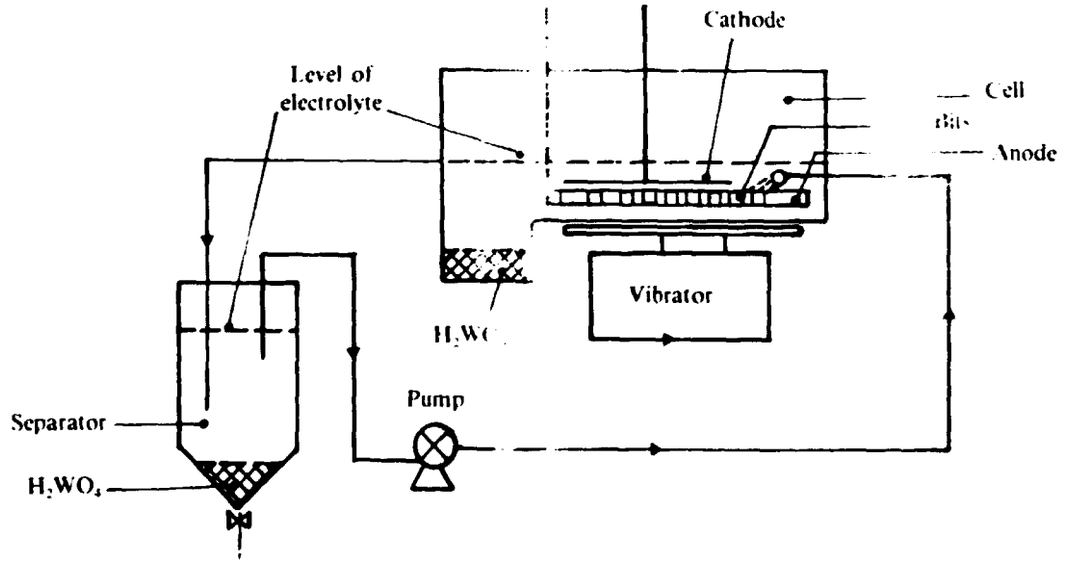


FIGURE 5. Layout of perforated-plate cell

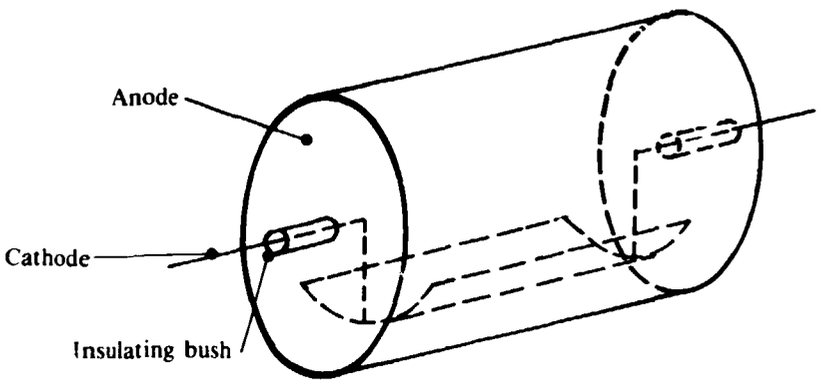


FIGURE 6. Modified rotary drum

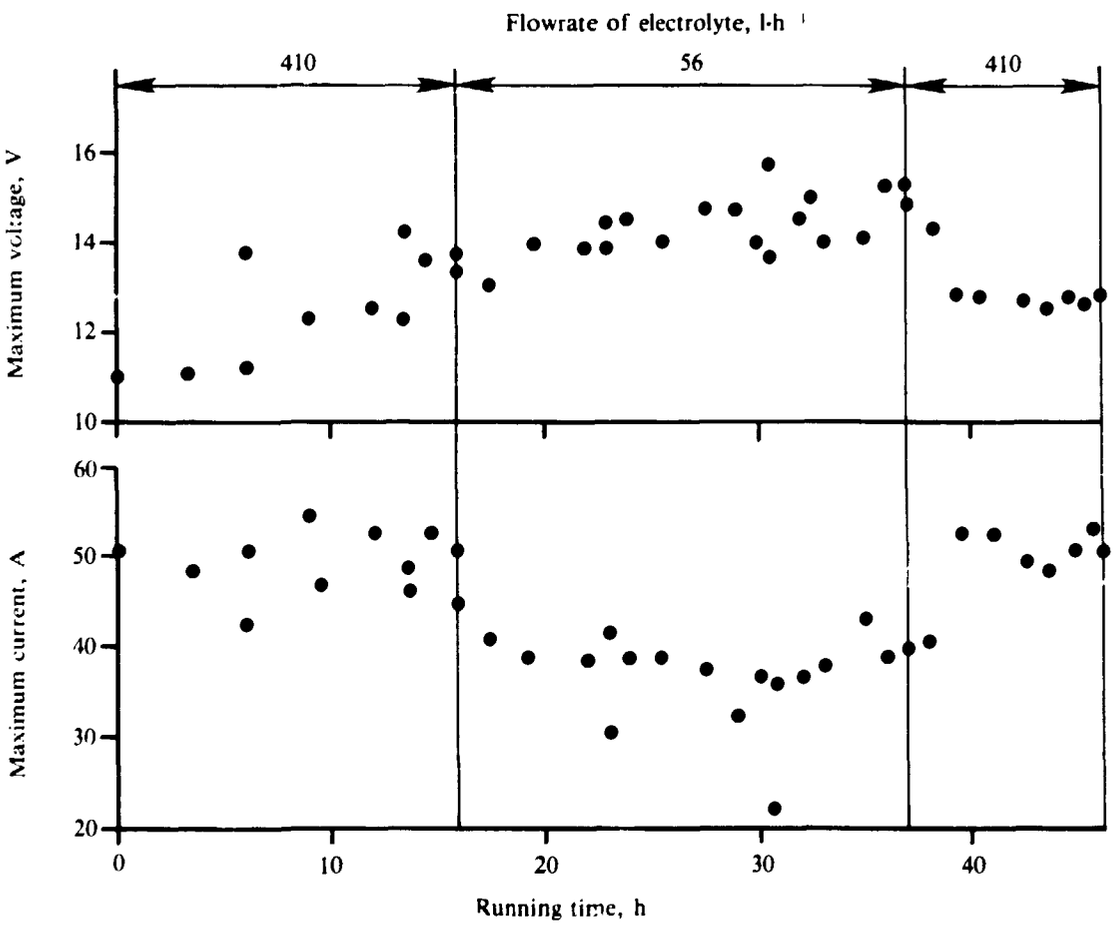


FIGURE 7. The effect of the flowrate of electrolyte on passivation in Run OC/3

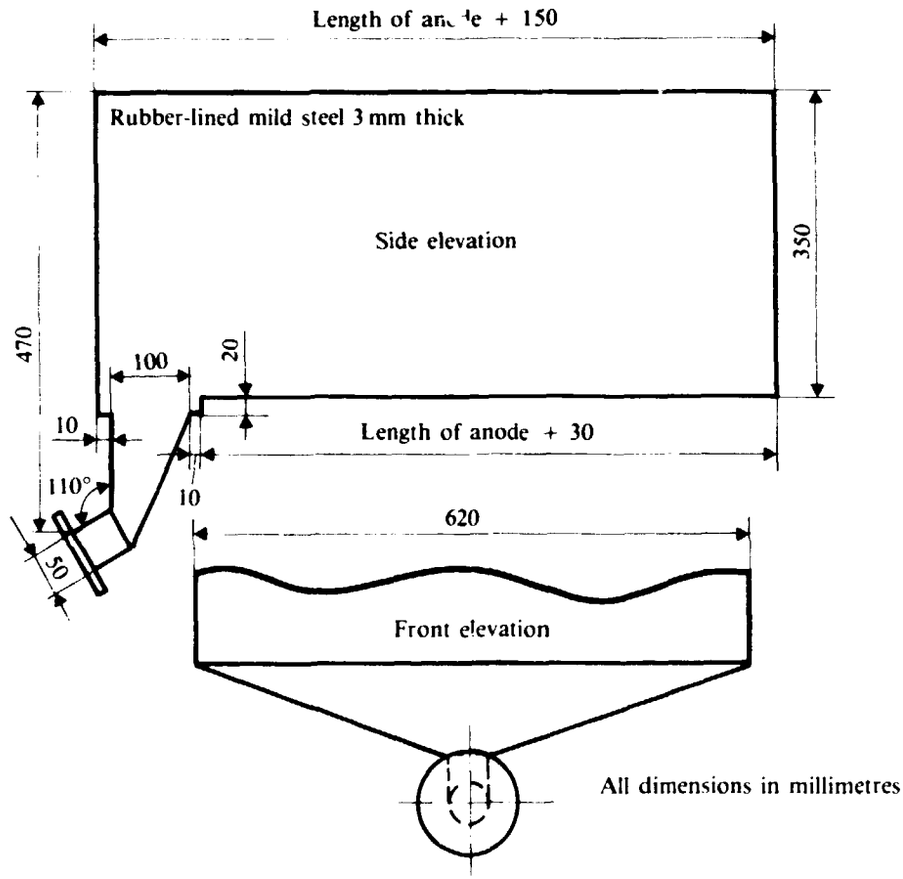


FIGURE 8. Front and side elevations of the pilot-plant cell

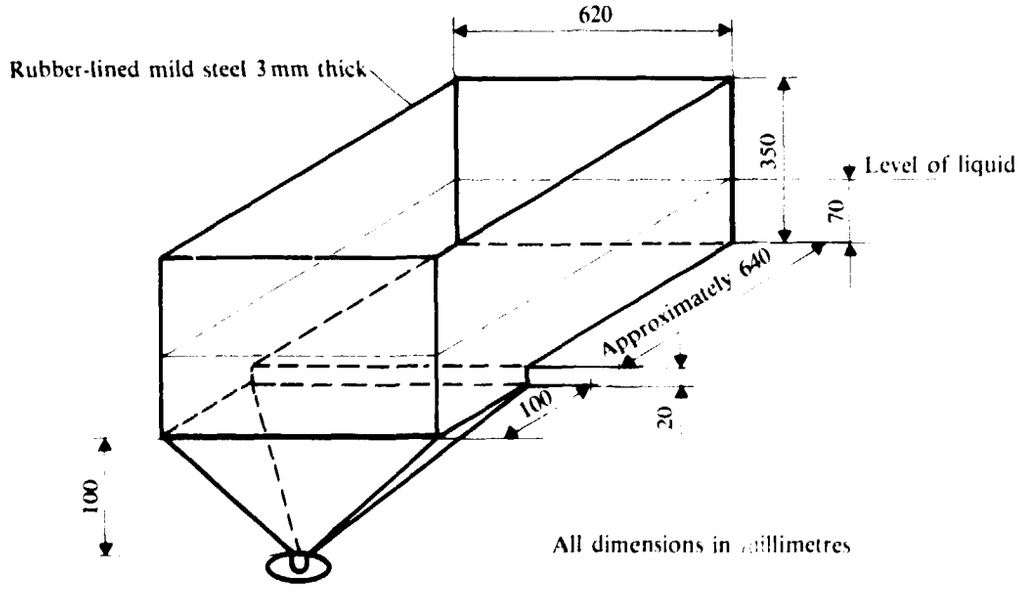


FIGURE 9. Oblique elevation of the pilot-plant cell

a

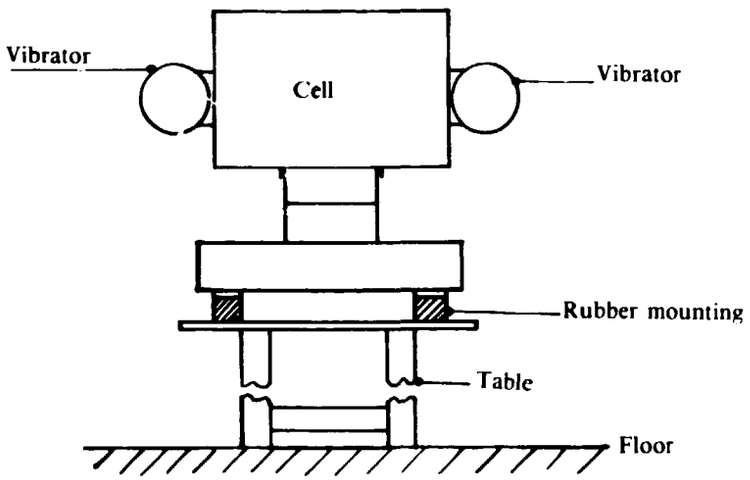


b

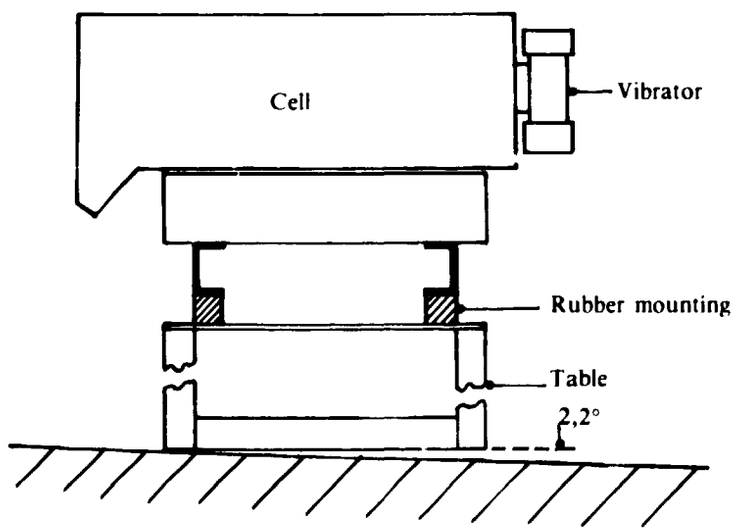


FIGURE 10. Overall view of the pilot-plant cell

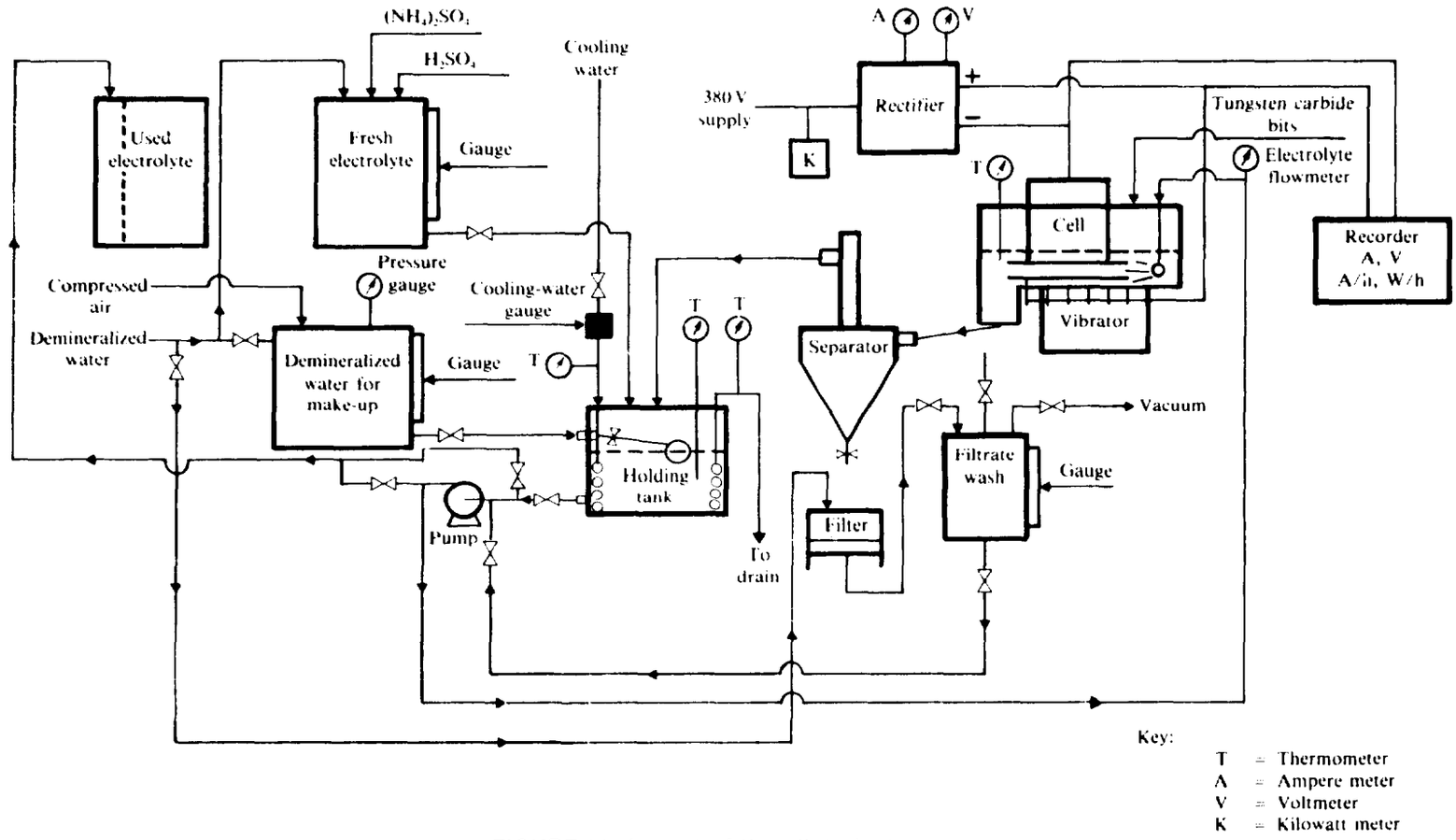


FIGURE 11. Layout of the pilot plant

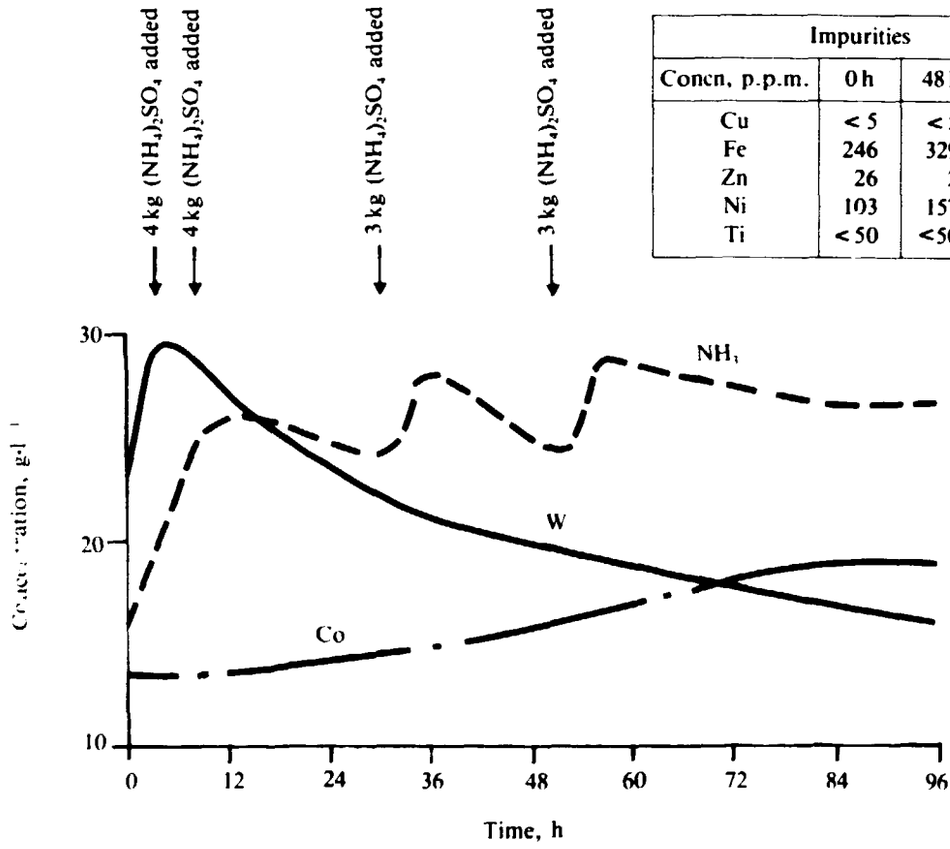


| Impurities | | | |
|---|---|---|---|
| Concn, p.p.m. | 0 h | 48 h | 96 h |
| Cu | < 5 | < 5 | < 5 |
| Fe | 246 | 329 | 472 |
| Zn | 26 | 2 | 3 |
| Ni | 103 | 157 | 208 |
| Ti | < 50 | < 50 | < 50 |

FIGURE 12. Concentration profile for Run 12P

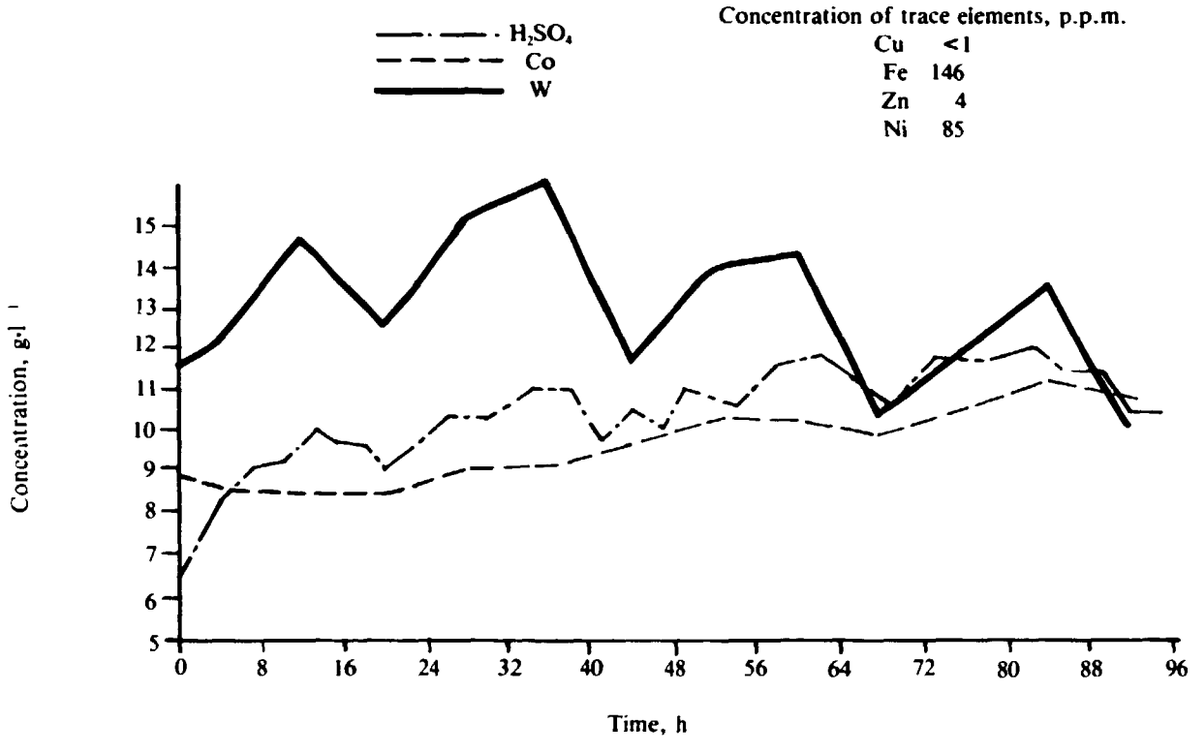


FIGURE 13. Concentration profile for Run 13P

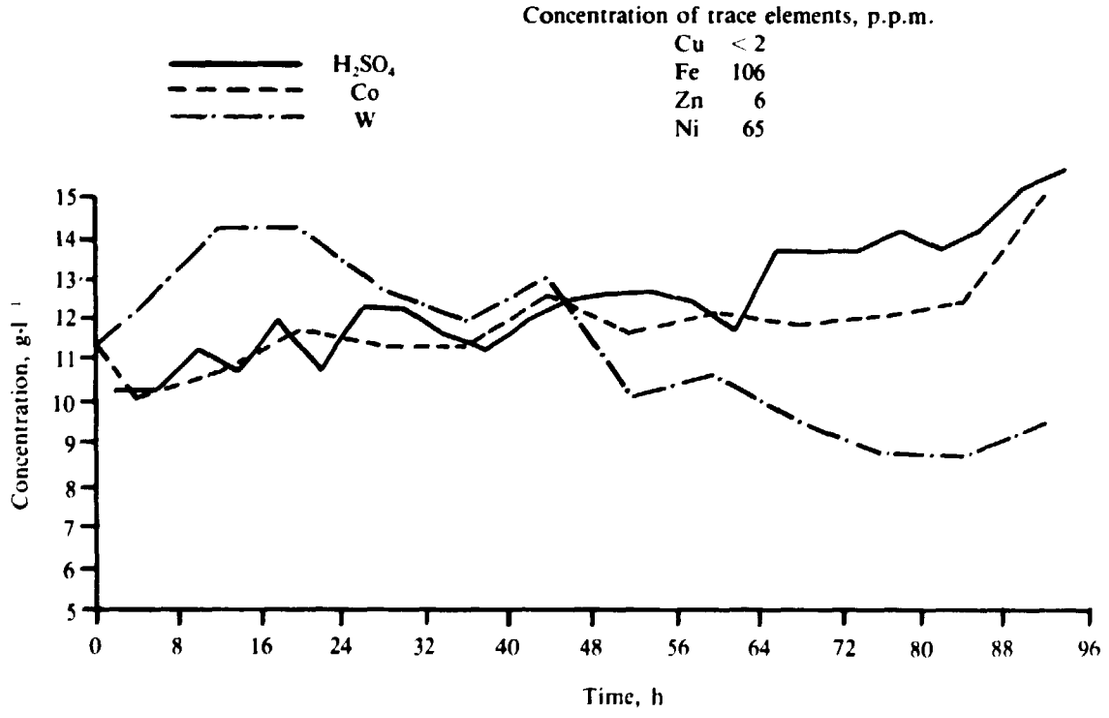


FIGURE 14. Concentration profile for Run 14P

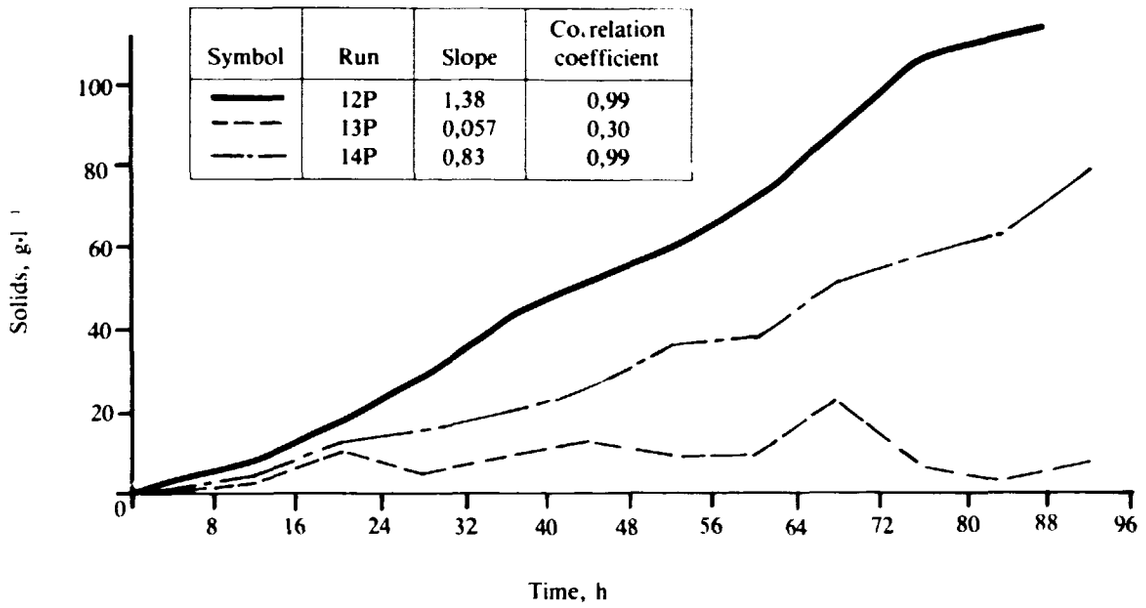


FIGURE 15. Build-up of solids in suspension

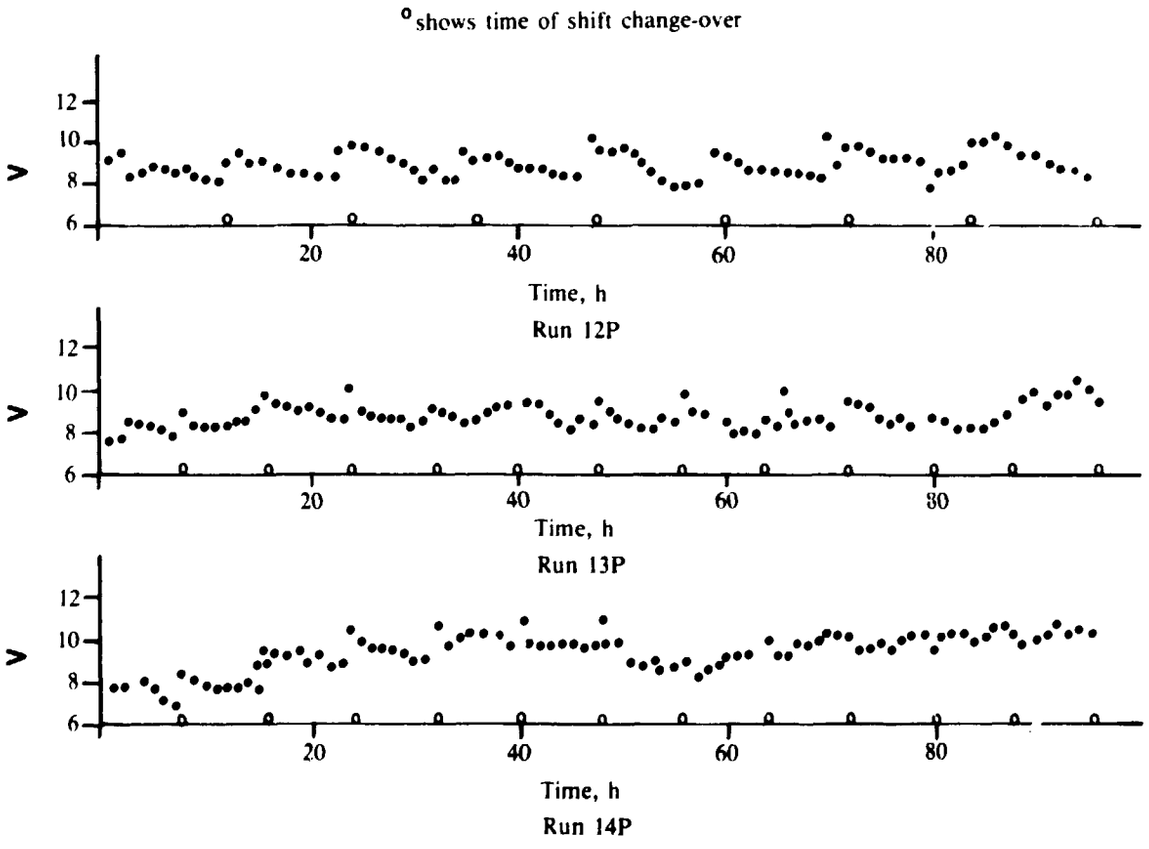


FIGURE 16. Voltage versus time for runs 12P, 13P, and 14P

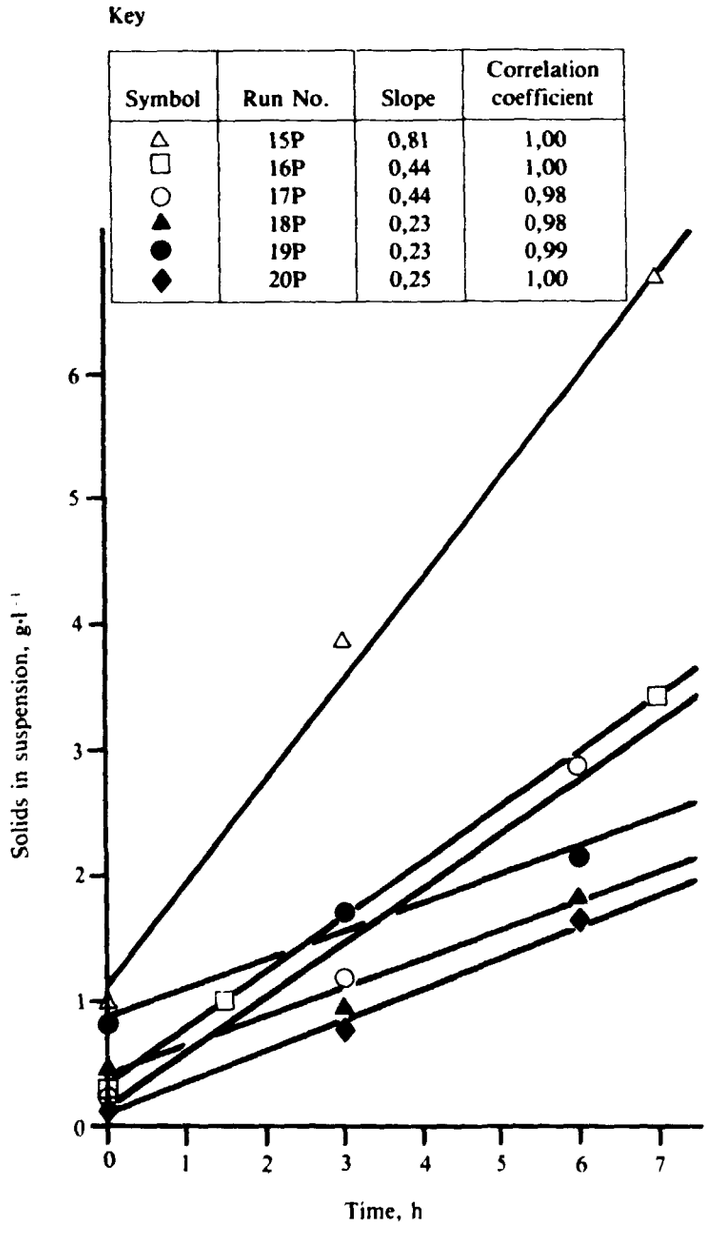


FIGURE 17. Increase of solids in suspension with time

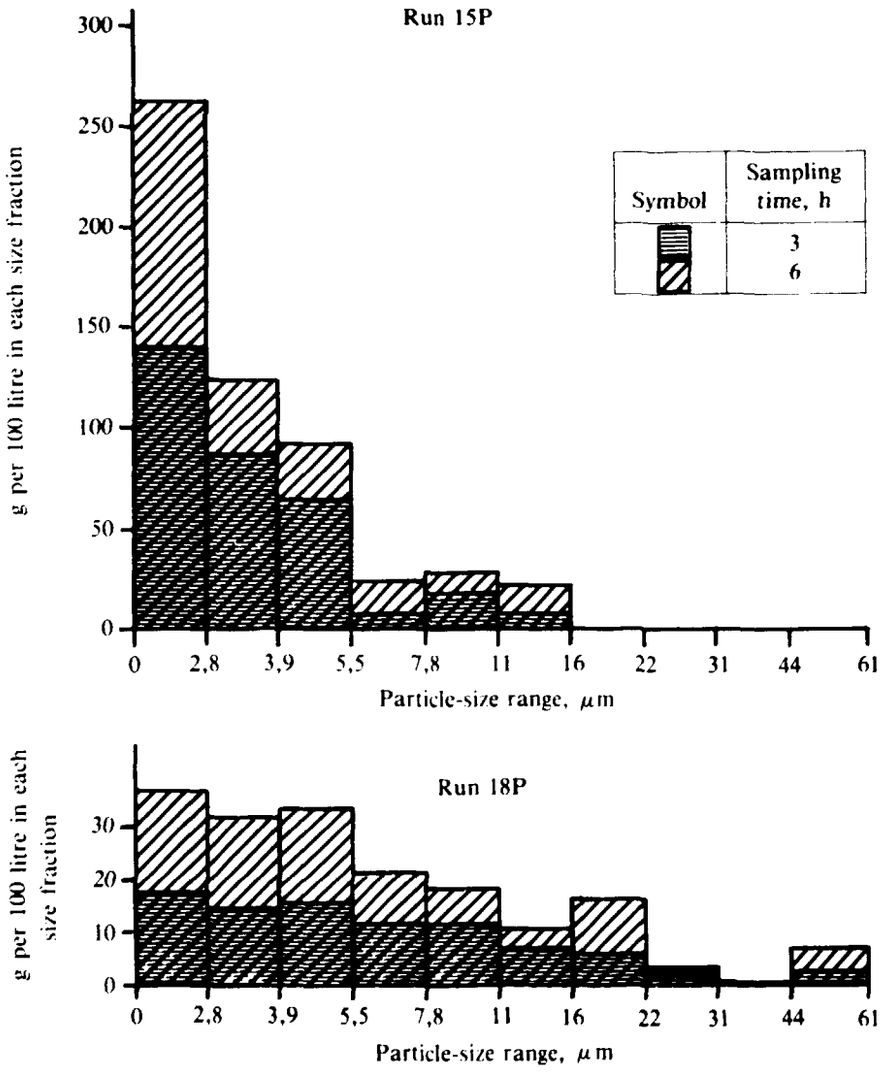


FIGURE 18. Histograms of particle size for Runs 15P and 18P

## APPENDIX

### CALCULATION OF THE REACTIONS IN THE PROCESS

The following reactions are assumed to occur in the process:

$$WC + 6H_2O \rightarrow H_2WO_4 + CO_2 + 10H^+ + 10e \quad \text{..... (1)}$$

$$TiC + 4H_2O \rightarrow TiO_2 + CO_2 + 8H^+ + 8e \quad \text{..... (2)}$$

$$TaC + 5H_2O \rightarrow 0{,}5Ta_2O_5{\cdot}H_2O + CO_2 + 9H^+ + 9e \quad \text{..... (3)}$$

$$Co \rightarrow Co^{2+} + 2e \quad \text{..... (4)}$$

From the compositions of machine-grade carbide (90 per cent tungsten carbide and 10 per cent cobalt by mass) and tool-grade carbide (70 per cent tungsten carbide, 10 per cent titanium carbide, 10 per cent tantalum carbide, and 10 per cent cobalt by mass) and a known feed (in this case a 3:1 blend by mass of machine-grade and tool-grade carbide), the mole fractions, $x_i$, of the various components were calculated:

$$x_{WC} = 0{,}659$$

$$x_{TiC} = 0{,}063$$

$$x_{TaC} = 0{,}020$$

$$x_{Co} = 0{,}258$$

The total current, $I$, is equal to the sum of the various partial currents, i.e.,

$$I = I_{WC} + I_{TiC} + I_{TaC} + I_{Co} \quad \text{..... (5)}$$

The molar rate of carbide consumption, $dm/dt$, is related to the current by the relationship

$$I = nF{\cdot}(dm/dt),$$

where $F$ is the Faraday constant, and $n$ is the number of electrons involved in the reaction. The number of electrons can be calculated from equations (1) to (4) and the mole fractions of each component, i.e.,

$$I = (10x_{WC} + 8x_{TiC} + 9x_{TaC} + 2x_{Co})F\frac{dm}{dt}. \quad \text{..... (7)}$$

The partial current of any component, for example $I_{Co}$, can be calculated from equations (5) and (7):

$$I_{Co} = \frac{2x_{Co}(dm/dt)}{(10x_{WC} + 8x_{TiC} + 9x_{TaC} + 2x_{Co})\, dm/dt} \cdot I$$

$$= 0{,}66\ I.$$

Similarly, $I_{WC} = 0{,}846\ I$

$$I_{TiC} = 0{,}065\ I$$

$$I_{TaC} = 0{,}023.$$

The hourly rate of oxidation of any component, for example $R_{Co}$, can be calculated from the partial currents and equation (6), i.e.,

$$R_{Co} = \frac{58{,}93 \times 3600 \times I_{Co}}{2IF}$$

$$= 0{,}070\,\text{g·A}^{-1}.$$

Similarly, $R_{WC} = 0{,}597\,\text{g·A}^{-1}$

$$R_{TiC} = 0{,}018\,\text{g·A}^{-1}$$

$$R_{TaC} = 0{,}018\,\text{g·A}^{-1}.$$

Hence the total nourly rate of carbide oxidation will be $0{,}703\,\text{g·A}^{-1}$. The hourly rate of oxide production can be calculated from equations (1) to (3), i.e.,

$$R_{H_2WO_4} = 0{,}761\,\text{g·A}^{-1}.$$

$$R_{TiO_2} = 0{,}024\,\text{g·A}^{-1}.$$

$$R_{Ta_2O_5} = 0{,}012\,\text{g·A}^{-1}.$$

Hence the total hourly rate of oxide production is

$$0{,}806\,\text{g·A}^{-1}.$$

The maximum theoretical solubility of the oxide in ammonia is 94 per cent.